https://doi.org/10.5194/se-2021-95
Preprint. Discussion started: 2 August 2021

Solid Earth
Discussions
Open Access
EGU

Variscan structures and their control on latest to post-Variscan basin architecture; insights from the westernmost Bohemian Massif and SE Germany

Hamed Fazlikhani, Wolfgang Bauer and Harald Stollhofen

GeoZentrum Nordbayern, Friedrich-Alexander-Universität (FAU) Erlangen-Nürnberg, Schlossgarten 5
5, 91054 Erlangen, Germany.
Corresponding author: Hamed Fazlikhani, hamed.fazli.khani@fau.de

Abstract

The Bohemian Massif exposes structures and metamorphic rocks remnant from the Variscan Orogeny in Central Europe and is bordered by the Franconian Fault System (FFS) to the west. Across the FFS, possible presence of Variscan units and structures are buried by Permo-Mesozoic sedimentary rocks. We integrate existing DEKORP 2D seismic reflection, well and surface geological data with the newly acquired FRANKEN 2D seismic survey to investigate the possible westward continuation of Variscan tectonostratigraphic units and structures, and their influence on latest to post-Variscan basin development. Subsurface Permo-Mesozoic stratigraphy is obtained from available wells and are tied to seismic reflection profiles using a synthetic seismogram calculated from density and velocity logs. Below the sedimentary cover, three main basement units are identified using seismic facies descriptions that are compared with seismic reflection characteristics of exposed Variscan units east of the FFS. Our results show that Upper Paleozoic low-grade metasedimentary rocks and possible Variscan nappes are bounded and transported by Variscan shear zones to ca. 65 km west of the FFS. Basement seismic facies in the footwall of the Variscan shear zones are interpreted as Saxothuringian basement. We show that the location of normal fault-bounded latest to post-Variscan Upper Carboniferous-Permian basins are controlled by the geometry of underlying Variscan shear zones. Some of these Upper Carboniferous-Permian normal faults reactivated as steep reverse faults during the regional Upper Cretaceous inversion. Our results also highlight that reverse reactivation of normal faults gradually decreases west of the FFS.

1. Introduction

Variscan orogenic units and structures in central and western Europe are extensively studied from disconnected exposed terranes in the Bohemian Massif, the Rheno-Hercynian Massif, the Black forest and Vosges, the Armorican Massif and the Central Iberian Zone (Franke, 2000). Between exposed Variscan units, sedimentary rocks obscure direct observation of possible lateral extension and architecture of Variscan tectonostratigraphy and structures. In southern Germany, for instance, Variscan units of the Bohemian Massif are correlated with exposed Variscan units in the Black forest and Vosges, ca. 300 km apart from each other, causing uncertainties in the lateral continuation and architecture of the Variscan tectonometamorphic Saxothuringian and Moldanubian zones, originally defined by (Kossmat, 1927). Although few wells provide local but valuable information about basement rock types, only few regional 2D seismic profiles (DEKORP 84-2s and 90-3B/MVE and KTB84) image the Variscan units and structures below the sedimentary cover between the Bohemian Massif and Black Forest exposures (Franke et al., 2017; Behr and Heinrichs, 1987; Wever et al., 1990; Edel and Weber, 1995; Meissner et al., 1987; Lüschen et al., 1987).

The recently acquired FRANKEN 2D seismic survey is covering the Carboniferous-Permian Kraichgau and Naab basins (Paul and Schröder, 2012; Sitting and Nitsch, 2012) and the overlying late Permian to Triassic Franconian Basin (Freudenberger and Schwerd, 1996) in the western vicinity of Bohemian Massif in SE Germany (Fig. 1). The FRANKEN survey is tied to the DEKORP 3/MVE-90 profile creating a

https://doi.org/10.5194/se-2021-95
Preprint. Discussion started: 2 August 2021


Solid Earth
Discussions
Open Access
EGU

grid of regional seismic reflection profiles imaging exposed and buried Saxothuringian units and structures of the Variscan Orogeny across the Franconian Fault System (FFS, Fig. 1). In this study we investigate the potential westward extension of Variscan tectonic units and structures and construct a first order relationship between Variscan and post-Variscan structures and basin development. Four new seismic profiles of the FRANKEN survey are interpreted utilizing subsurface and surface geological data and are tied to the existing DEKORP-3/MVE-90 profile. Underneath the Permo-Mesozoic sedimentary cover three main Basement Seismic Facies (BSF1-3) are identified, based on lateral and vertical changes in reflection amplitude and connectivity. Comparing seismic reflection patterns observed in exposed Variscan rocks of Bohemian Massif with reflection patterns along the FRANKEN seismic profiles we show a W-SW continuation of Variscan shear zones and associated Variscan allochthons. The control of Variscan shear zone geometry in strain localization and latest to post-Variscan basin development and brittle fault interactions are discussed.

2. Geological setting

2.1. Variscan geodynamics and tectonic framework

The Bohemian Massif comprises remnants of the Upper Paleozoic collision of Laurussia and Gondwana, known as Variscan Mountain Belt, and of the pre-Variscan basement in Central Europe (Franke, 2000; Kroner et al., 2007). The Variscan Orogeny has resulted in a wide range of metamorphic units, ranging from high-pressure and high-temperature metamorphic to low-grade metasedimentary rocks, abundant granitic intrusives and crustal-scale shear zones and faults. From north to south, the Variscides have traditionally been subdivided into three main tectonometamorphic zones, the Rhenohercynian, Saxothuringian (including the Mid-German Crystalline High) and Moldanubian (Kossmat, 1927; Franke, 2000; Kroner et al., 2007). Saxothuringian and Moldanubian rocks are well exposed in the Bohemian Massif, but buried by Palaeozoic and Mesozoic sediments towards the west.

The Saxothuringian zone, as the main area of interest, underwent three main deformational phases during the Variscan Orogeny (Kroner et al., 2007). A first deformation phase (D1) developed before 340 Ma and records pervasive deformation during the subduction and collision resulting in the development of recumbent folds and thrusts with top-to-the-southwest transport direction as evidenced by kinematic indicators (Kroner et al., 2007; Scwan, 1974; Stettner, 1974; Franke et al., 1992). A second deformation phase (D2) developed due to the exhumation and juxtaposition of High-pressure and Ultra high-pressure metamorphic rocks in the upper crust and a ca. 45° stress rotation after 340 Ma. The D2 deformation phase is manifested by dextral transpression and ductile deformation with a top-to-the-northwest transport direction (Kroner et al., 2007; Franke and Stein, 2000; Kroner and Goerz, 2010; Franke, 1989). A third deformation phase (D3) records latest Variscan tectonics at ~320 Ma and is represented by the folding of synorogenic deposits during general NW-SE to NNW-SSE shortening (Hahn et al., 2010). D3 is dominated by a wrench tectonic phase and the collapse of thickened crust, resulting in the development of dextral strike-slip faults initiating fault-bounded graben and half-graben basins in Central Europe, including the study area in SE Germany (Schröder, 1987; Arthaud and Matte, 1977; Krohe, 1996; Stephan et al., 2016; Peterek et al., 1996b; Ziegler, 1990). Detailed and comprehensive overviews of the geodynamic and tectonostratigraphic evolution of the Mideuropean Variscides have been presented by (Linnemann and Romer, 2010; Franke et al., 2000).

During earliest post-Variscan development at <305 Ma wide-spread intermontane Late Carboniferous-Permian fault bounded graben and half-graben basins, such as the NE-SW trending Saar-Nahe (Henk, 1993; Stollhofen, 1998; Boy et al., 2012) Saale (Ehling and Gebhardt, 2012), Kraichgau and Schramberg basins (Sitting and Nitsch, 2012) and NW-SE striking basins (e.g. Naab and Thuringian Forest basins) are formed (Paul and Schröder, 2012; Lützner et al., 2012). Compared to the Carboniferous, the Rotliegend is characterized by widespread intrabasinal volcanism and depositional areas became enlarged across the internal parts of the Variscan Belt, e.g. in Switzerland (Matter et al., 1987), France

https://doi.org/10.5194/se-2021-95
Preprint. Discussion started: 2 August 2021

(Chateauneuf and Farjanel, 1989; Cassinis et al., 1995; Engel et al., 1982; Laversanne, 1978; McCann et al., 2006), Germany (Henk, 1993; Stollhofen, 1998; Boy et al., 2012; Lützner et al., 2012; Sitting and Nitsch, 2012; Paul and Schröder, 2012) and Iberia (e.g. (Cassinis et al., 1995). In the study area, Carboniferous-Permian units are only exposed along the Franconian Fault System (FFS, also known as Franconian Line), but are drilled by several wells located farther west, in the Kraichgau and Naab basins (Fig. 1, Table 1).

In general, the Saxothuringian basement units beneath the sedimentary cover show a smooth topography with a gentle southward rise, including topo lows along the SW-NE axis Würzburg-Rannungen and along the NW-SE axis Staffelstein-Obernsees, the latter subparallel to the FFS (Gudden, 1981; Gudden and Schmid, 1985). Saxothuringian basement lithologies drilled by wells Wolfersdorf and Mittelberg in the north, well Eltmann to the west and well Obernsees in the southeast of the study area (Fig. 1 and Table 1) are Upper Devonian to Lower Carboniferous low-to medium-grade metasedimentary rocks (Hahn et al., 2010; Stettner and Salger, 1985; Trusheim, 1964; Specht, 2018; Friedlein and Hahn, 2018).

2.2. Latest to Post-Variscan stratigraphic and structural architecture

Carboniferous-Permian units in the study area dominantly comprise of clastic continental sediments deposited in fault bounded basins outcropping in the Schalkau, Stockheim, Rugendorf, Wirsberg and Weidenberg areas (Schröder, 1987). Thicknesses are highly variable ranging from about 100 m to >700 m in the Kraichgau Basin and from about 100 m up to >1400 m in the Naab Basin adjacent to the FFS (Gudden, 1981; Paul and Schröder, 2012). At Stockheim outcrop, well Wolfersdorf drilled into 726 m Rotliegend, excluding an unknown amount of eroded section (Table 1). In the center of the study area, 109 m of Rotliegend are encountered by well Mürsbach 1 (Gudden, 1981), whereas wells Mürsbach 6 and Staffelstein 1 only drilled ca. 20 and 43 m of the upper parts of the Rotliegend (Table 1). Well Eltmann, located in a basin marginal position, encountered only 3 m Rotliegend (Table 1, (Trusheim, 1964). Towards the SE of the study area well Obernsees encountered 18.3 m of Rotliegend overlaying the metasedimentary basement rocks (Table 1, (Helmkampf, 2006; Ravidà et al., 2021). However, ca. 19 km NE of well Obernsees, well Lindau 1 drilled 250.25 m of Rotliegend strata without reaching the Rotliegend base (Fig. 1, Table 1, (Freudenberger et al., 2006). Compared to the Rotliegend, Zechstein thicknesses tend to be more uniform, mainly comprised of clay- and sandstones, dolomites and thin layers of anhydrite (Schuh, 1985). Drilled Zechstein thicknesses are 117 m in well Eltmann, 126 m in well Mürsbach 1, and 107 m in well Staffelstein and 104.9 in well Obernsees (Table 1). Refraction seismic surveys in the south of the study area (Nürnberg area) proved the existence of deep, fault-bounded grabens, whereas the Rotliegend top is characterized by a peneplain beneath the Zechstein (Bader and Bram, 2001; Buness and Bram, 2001). This suggests a regional disconformity between Rotliegend and Zechstein and supports the separation between the Carboniferous-Permian (mainly Rotliegend) Kraichgau Basin and the post-Rotliegend (mainly Mesozoic) Franconian Basin development (c.f. (Freudenberger et al., 2006; Paul, 2006).

Triassic stratigraphy is divided into Lower to lowermost Middle Triassic Buntsandstein, the Middle Triassic Muschelkalk and the uppermost Middle to Upper Triassic Keuper Groups (STD, 2016), Fig. 2). Siliciclastic sandstones of the Buntsandstein Group are 572 m thick in well Staffelstein 1, 530.7 m in well Mürsbach 6, and 510 m in well Eltmann, decreasing to 417.15 m in well Obernsees in the southeast (Table 1, (Gudden, 1977; Emmert et al., 1985; Helmkampf, 2006). Buntsandstein units are exposed in fault blocks between the FFS and the Eisfeld-Kulmbach fault in the eastern part of the study area (Fig. 1). The Muschelkalk Group is dominated by carbonates, dolomites and few gypsum, 240 m thick in well Staffelstein 1, 210.7 m in well Mürsbach 6, and 236 m in well Eltmann, decreasing

https://doi.org/10.5194/se-2021-95
Preprint. Discussion started: 2 August 2021

140 southeastward to 178 m in well Obernsees (Table 1, (Gudden, 1977; Emmert et al., 1985). Muschelkalk
141 units crop out along the FFS and the Eisfeld-Kulmbach fault and also west of well Eltmann (Fig. 1). The
142 Keuper Group consists mainly of sandstones that are 530.2 m thick in well Staffelstein 1, 532 m in well
143 Staffelstein 2, decreasing southeastward to 483 m in well Obernsees (Franz et al., 2014; Gudden, 1977;
144 Emmert et al., 1985). Keuper units are broadly exposed in the western and northwestern part of the
145 study area and in the fault block bounded by the Eisfeld-Kulmbach and Asslitz faults (Fig. 1). Jurassic
146 units preserved in the central and eastern parts of the study area, but eroded towards the west and
147 northwest (Fig. 1). Jurassic outcrops to the east are fault bounded and are limited to the footwall of
148 Eisfeld-Kulmbach, Asslitz and Lichtenfels reverse faults (Fig. 1). The Jurassic interval is 102-104 m thick
149 in wells Staffelstein 1 & 2 in the north and 140 m thick in well Obernsees in the SE (Table 1, (Meyer,
150 1985; Gudden, 1977). Cretaceous sedimentary rocks are preserved in the central and southeastern
151 parts of the study area (Fig. 1).

152 The structural architecture of the eastern study area is characterized by ten to hundreds of kilometer
153 long NW-SE striking multi-segmented reverse faults (e.g. Eisfeld-Kulmbach and Asslitz faults), whereas
154 towards the west only normal faults (e.g. Bamberg fault, Kissingen-Haßfurt fault zone) are developed
155 (Fig. 1). The NW-SE Franconian Fault System (FFS) is the dominant structural feature, representing the
156 tectonic contact between the western Bohemian Massif to the east and the Late Permian to Mesozoic
157 Franconian Basin to the west (Fig. 1). The FFS initiated most likely during latest Variscan tectonics and
158 has been reactivated at least during Early Triassic and Cretaceous times (Carlé, 1955; Freyberg, 1969;
159 Peterek et al., 1997; Wagner et al., 1997). FFS's total amount of hangingwall uplift is estimated ca.
160 5500 m, as evidenced by titanite and apatite fission-track ages, the sericite K-Ar ages of fault rocks and
161 the sedimentary strata adjacent to the fault (Wemmer, 1991; Wagner et al., 1997; Peterek et al.,
162 1997). Sub-parallel to and ca. 9 km SW of FFS, the NE dipping Eisfeld-Kulmbach Fault mainly exposes
163 Lower and Middle Triassic units on its hangingwall side (Fig.1). In the SE and the central footwall of
164 the Eisfeld-Kulmbach Fault, Upper Triassic and Lower Jurassic units are crop out while laterally to the
165 NW Middle and Lower Triassic and some Permian units (Schalkau outcrop) are exposed (Fig.1). Farther
166 SW in the footwall of Eisfeld-Kulmbach Fault, the Asslitz Fault can be traced over ca. 50 km, exposing
167 Upper Triassic units in its hanging wall (Fig. 1). The most westward major reverse fault is the Lichtenfels
168 Fault, mapped over ca. 16 km at the surface (Fig. 1).

169 West and southwest of the Lichtenfels Fault, the structural architecture of the study area is dominated
170 by NW-SE normal faults such as the Staffelstein and Bamberg faults and the prominent Kissingen-
171 Haßfurt and Heustreu fault zones (Fig. 1). Studies of regional upper crustal paleostress patterns reveal
172 constant changes in stress field orientations since the Palaeozoic comprising normal faulting and both,
173 extensional and compressional strike-slip faulting implying multiple fault reactivation (Peterek et al.,
174 1996a; Peterek et al., 1997; Bergerat and Geyssant, 1982; Coubal et al., 2015; Navabpour et al., 2017;
175 Eynatten et al., 2021).

176

177 **3. Data and methods**
178 **3.1. FRANKEN seismic reflection acquisition and recording parameters**

179 The FRANKEN 2D seismic survey is comprised of four seismic lines, with a total line length of 230.8 km.
180 The survey area is situated in northern Bavaria, SE Germany covering an area of approximately 90 km
181 x 45 km (Fig. 1). The FRANKEN seismic survey was designed to cross deep wells and image the upper
182 crustal levels in northern Bavaria. Together with existing DEKORP, KTB and OPFZ it constitutes a grid
183 of 2D seismic reflection profiles, crossing major structural elements. FRANKEN-1801 and 1803 lines
184 are striking NW-SE perpendicular to FRANKEN-1802 and 1804 profiles (Fig. 1). Profile FRANKEN-1803

https://doi.org/10.5194/se-2021-95
Preprint. Discussion started: 2 August 2021

links to the DEKORP-3/MVE-90 profile in the NW and to the OPFZ-9301 profile towards the SE (Fig. 1). FRANKEN-1802 and 1804 strike NE-SW and are perpendicular to the major fault zones. Table 2 summarizes acquisition and processing parameters of the FRANKEN seismic survey.

3.2 Seismic interpretation methods

In this study we integrate information from 9 deep wells (1100-1600 m) and surface geology to interpret the newly acquired FRANKEN seismic reflection survey in SE Germany. Available wells are mainly located in the center and the western part of the study area (Fig. 1 and Table 1). Seismic-well tie and time-depth relationships are established using sonic velocity and density logs of the Mürsbach 1 well (Gudden, 1971). The calculated synthetic seismogram is correlated with the real seismic traces at the well location and enabled us to transfer geological, in particular stratigraphic information from the well to the intersected seismic profiles (Fig. 2). Horizon interpretation started from the profile FRANKEN-1802 at the well Mürsbach-1 location where the best seismic-well tie has been established. Interpretation of stratigraphic markers was then extended from the profile FRANKEN-1802 to other intersecting profiles. In the sedimentary cover, seismo-stratigraphic facies and seismic characters are defined, based on the lateral and vertical changes in seismic amplitudes, reflectivity and coherency. Observed formation tops in wells in combination with defined seismo-stratigraphic facies are used in the seismic horizon interpretation especially where there is no well available. Below the sedimentary cover three main seismic facies are identified and are used to characterize and interpret basement units.

3.3 Seismo-stratigraphic facies

Characteristic seismic signatures of stratigraphic intervals drilled by wells and observed in the FRANKEN survey are described for the Permo-Mesozoic interval. Upper Mesozoic-Cretaceous units are only locally preserved in the study area and are not drilled by any of the deep wells, restricting the interpretation of the Jurassic-Cretaceous boundary and the description of their seismic signature. Jurassic strata show a medium amplitude and semi-continuous reflections (Fig. 3A). The Jurassic-Triassic boundary is marked by the appearance of slightly higher amplitudes and rather continuous reflections in the Triassic compared to the overlying Jurassic interval (Fig. 3A). This boundary is correlated with the Staffelstein and Obernsees wells along profiles FRANKEN-1802 and 1803 respectively.

Upper Triassic Keuper units generally show continuous and medium to high amplitude reflections of alternating sandstones, siltstones and some gypsiferous units (Fig. 3B). Only the shallow marine dolomites (Grabfeld Fm.) at the base of the Keuper Group (Haunschild, 1985; Gudden, 1981) are characterized by high amplitudes and continuous pairs of reflections acting as regional marker reflection along all profiles (Fig. 3B). Middle Triassic Muschelkalk units are comprised of lime-, marl-, and dolostones, that are recorded by two distinct seismic facies in the study area, a semi-continuous and medium amplitude reflection with ca. 50 ms thick on top and continuous and high amplitude reflections at the bottom (Fig. 3C). The sandstone dominated Buntsandstein Group is characterized by semi-continuous and rather medium energy amplitudes that gradually show slightly higher energy and continuity of reflections towards the top (Fig. 3D). A continuous and very high amplitude reflection defines the Permian-Triassic boundary between the Buntsandstein and the underlying Zechstein Group (Fig.3D). The latter shows ca. 25-30 ms of continuous and high amplitude reflections which are correlated to an anhydrite and dolomite bearing interval in the upper part of the Zechstein (Gudden, 1977; Schuh, 1985; Gudden and Schmid, 1985). Below the Zechstein high amplitude reflections, semi-continuous and medium amplitude reflections of the Rotliegend occur (Fig. 3E). These reflections represent the upper parts of the Rotliegend and gradually become less reflective and discontinuous

https://doi.org/10.5194/se-2021-95
Preprint. Discussion started: 2 August 2021

with depth with some reflections being only locally present and laterally becoming less reflective and partly transparent (Fig. 3E, 4A & B). The boundary between the sedimentary cover and the pre-Permian low- to medium grade metasedimentary rocks (hereafter considered as basement) is drilled by wells Wolfersdorf and Mittelberg in the north, well Eltmann to the west and the well Obernsees to the southeast and is not particularly reflective in the seismic survey (Table 1 and Fig. 4A & B). However, at some locations semi-continuous and low energy reflections of the Rotliegend can be distinguished from discontinuous but slightly higher energy reflections below, interpreted as a transitional zone between sedimentary cover and underlying metasedimentary rocks (Fig. 4A & B).

3.4 Basement seismic facies

Basement units below the sedimentary cover comprise three seismic facies, based on observed differences in reflectivity, frequency and continuity of reflections.

3.4.1 Basement Seismic Facies 1 (BSF1)

Basement Seismic Facies 1 (BSF1), consists of discontinuous, low amplitude and low frequency reflections that become transparent at some locations (Figs. 4A & B). Higher amplitude and semi-continuous reflections of the Rotliegend progressively transform into BSF1 without a seismically detectable boundary (Fig. 4B). The thicknesses of BSF1 units generally thin westward and reach 2.5 s TWT at their deepest position. BSF1 is sampled by well Eltmann where 94 m of (?Devonian) quartzites and metasedimentary rocks are described (Trusheim, 1964), whereas well Obernsees cored 48.3 m of ?Late Paleozoic metasedimentary rocks (Table 1, (Trusheim, 1964; Stettner and Salger, 1985). Farther north well Mittelberg drilled into 100.5 m of Upper Devonian-Lower Carboniferous rocks below the Rotliegend (Table 1, (Friedlein and Hahn, 2018; Hahn et al., 2010). These Upper Devonian-Lower Carboniferous rocks (Gleitsch Formation) are interpreted as syn-Variscan inner shelf facies sedimentary rocks (Thuringian facies), low grade metamorphosed during the Variscan Orogeny (Hahn et al., 2010; Kroner et al., 2007). Albeit well Mittelberg is not tied to seismic profiles it additionally confirms the presence of low grade metasedimentary rocks below the Rotliegend.

In the FFS hangingwall, Münchberg nappe units (Variscan allochthon) are transected by the DEKORP85-4N and DEKORP-3/MVE-90 seismic profiles (Figs. 1 and 5). Münchberg nappe units are surrounded by low grade metasedimentary rocks of outer shelf facies (Bavarian facies) and inner shelf facies (Thuringian facies) as described by (Gümbel, 1879; Linnemann et al., 2010; Heuse et al., 2010). Exposed nappe units and low grade metasedimentary rocks show discontinuous to semi-continuous and low amplitude reflections, similar to BSF1 of the FRANKEN survey in the FFS footwall (Fig. 5). Similar low amplitude and low frequency reflections of BSF1 are also observed at the NW end of the DEKORP85-4N profile (Fig. 5A & B). There, these reflections are associated with low-grade Lower Carboniferous Flysch deposits (inner and outer shelf facies) exposed at the surface (DEKORP Research Group, 1994a). Based on seismic facies description and in the lack of well information, differentiation between allochthons, flysch sedimentary rocks, inner and outer shelf facies is ambiguous. BSF1 is therefore interpreted as the W-SW extension of low-grade inner and outer shelf facies, low-grade Lower Carboniferous flysch sedimentary rocks and possible Variscan allochthons (DEKORP Research Group, 1994b). Correlating with exposed basement units E-NE of the FFS, these units are interpreted to represent the W-SW extension of the Ziegenrück-Teuschnitz Syncline of the Saxothuringian zone.

3.4.2 Basement Seismic Facies 2 (BSF2)

https://doi.org/10.5194/se-2021-95
Preprint. Discussion started: 2 August 2021


Solid Earth
Discussions
Open Access
EGU

High amplitude, continuous and dipping reflection packages are bounding BSF1 at depth and are defined as Basement Seismic Facies 2 (BSF2, Fig. 4A, C and 5). BSF2 reflections are not drilled by wells within the survey area, however, similar reflections observed along reprocessed DEKORP85-4N and DEKORP-3/MVE-90 profiles below BSF1 are exposed at the surface and represent highly sheared rocks including phyllites developed during Variscan tectonics (Fig. 5, (DEKORP and Orogenic Processes Working Group, 1999; Franke and Stein, 2000). We interpret BSF2 as Variscan detachment/shear zones translating and involving low-grade inner and outer shelf facies, low-grade Lower Carboniferous flysch sedimentary rocks and Variscan nappes. BSF2 therefore includes the upper parts of the Saxothuringian parautochthonos (highly sheared parts of inner shelf facies) and lower parts of allochthons involved in Variscan tectonics. Similar intrabasement, high amplitude and dipping reflections are interpreted as orogenic and postorogenic shear zones in the Norwegian Caledonides (Phillips et al., 2016; Fazlikhani et al., 2017; Wrona et al., 2020), offshore Brazil (Strugale et al., 2021; Vasconcelos et al., 2019), offshore New Zealand (Collanega et al., 2019), and in the South China Sea (Ye et al., 2020). High amplitude and continuous reflections of BSF2 below the Münchberg nappe and across the FFS to the west are therefore interpreted as the W-SW extension of a Variscan detachment/shear zone transporting allochtonous nappes and underlying metasedimentary rocks W-SW, towards the Franconian Basin area. BSF2 reflections generally get shallower from east to west and reach to the base of the overlying sedimentary units.

3.4.3 Basement Seismic Facies 3 (BSF3)

Basement Seismic Facies 3 (BSF3) is characterized by semi-continuous and medium-amplitude reflections (Fig. 4A & D). BSF3 is bounded by BSF2 at the top and extends to the lower limit of the dataset at 8 s TWT. BSF3 does not show any preferential dip direction and locally hosts some higher amplitude, continuous and dipping reflections of BSF2. Such high amplitude reflections of BSF2 are branching off the main BSF2 packages or are developed at deeper levels and are interpreted as segments of major shear zones or locally developed shear zones during the Variscan tectonics. BSF3 is not drilled by wells, nevertheless considering the tectonostratigraphic position of BSF3 being below the Variscan detachment/shear zones (BSF2), BSF3 is interpreted to represent the lower parts of inner shelf facies (not involved in Variscan tectonics) and crystalline basement (Cadomian basement) of the Saxothuringian zone.

4 Seismic reflection Interpretation of the FRANKEN seismic survey

Described seismic facies in the sedimentary cover and underlying basement units and well information are utilized to interpret the FRANKEN seismic profiles.

4.1 Profile FRANKEN-1801

Profile FRANKEN-1801 is 47.9 km long and extends NW-SE from south of Bamberg to the NW of Haßfurt (Fig. 1). At the surface, mainly Keuper units are exposed (Fig. 1). Thicknesses of remnant Keuper units progressively decrease to the W-NW and at the northwestern edge of profile FRANKEN-1801, Muschelkalk units are exposed at the surface in the footwall of a segment of the Kissingen-Haßfurt Fault Zone (Fig. 6). This fault zone is mapped over ca. 60 km with ca. 7-10 km width, sub-parallel to the NW-SE striking FRANKEN-1801 profile (Fig. 1). Some segments of the Kissingen-Haßfurt Fault Zone are oblique and are imaged by the FRANKEN-1801 profile. Muschelkalk and Buntsandstein units are fairly tabular with no major lateral thickness changes (Fig. 6). Most of the interpreted faults (seismic scale) are normal faults, while major reverse faults are sub-parallel and are not imaged in profile FRANKEN-1801.

https://doi.org/10.5194/se-2021-95
Preprint. Discussion started: 2 August 2021


Solid Earth
Discussions
Open Access
EGU

316 Below the Buntsandstein, Permian deposits including 114 m Zechstein and 3 m Rotliegend are drilled
317 by well Eltmann, 2230 m to the NE of profile FRANKEN-1801 (Fig. 6) (Trusheim, 1964). Semi-continues
318 and medium-amplitude reflections below the Zechstein are interpreted as Rotliegend deposits (Fig.
319 6). As the Rotliegend base is not particularly reflective in the seismic reflection data, it is difficult to
320 interpret the top basement boundary. Towards the NW in the center of the FRANKEN-1801 profile,
321 BSF1 reflections (Paleozoic metasedimentary rocks and Variscan nappes) are present below the
322 Permian rocks and are underlain by a Variscan shear zone (BSF2, Fig. 6). From the SE, the Variscan
323 shear zone shallows to the NW and reaches ca. 700 ms TWT at the center of the profile (Fig. 6).

324 **4.2 Profile FRANKEN-1802**

325 Profile FRANKEN-1802 extends NE-SW with 47.7 km length (Fig. 1). This profile is at a high angle to the
326 prominent NW-SE faults, and therefore provides a good subsurface image of these structures (Fig. 7).
327 Profile FRANKEN-1802 is tied to the well Eltmann and is in the vicinity of wells Mürsbach 6 (630 m to
328 the S), Staffelstein 1 (1235 m, to the SE) and Staffelstein 2 (890 m, to the SE). Profile FRANKEN-1802
329 is used as the reference profile for the seismo-stratigraphic interpretation (Fig. 7). Jurassic rocks are
330 preserved in the footwall of the Mürsbach and Lichtenfels reverse faults drilled with 104 m thickness
331 by well Staffelstein 2 (Table 1; (Gudden, 1977). Keuper strata are exposed in the hanging wall of the
332 Lichtenfels Fault at the NE edge of profile FRANKEN-1802 (Fig. 7). Keuper is drilled with 532 m in
333 thickness by well Staffelstein 2. Towards the SW the Keuper is increasingly eroded and only 178.6 m
334 are preserved at the location of well Eltmann (Fig. 7 and Table 1, (Gudden, 1977; Trusheim, 1964).
335 Muschelkalk and Buntsandstein sedimentary rocks are tabular and regionally dip to the E-NE (Fig. 7).
336 The Zechstein is penetrated by wells Eltmann, Mürsbach 1 and 6, and Staffelstein 1 and is 103-121 m
337 thick (Table 1; (Gudden, 1985). Below the Zechstein units, Rotliegend is drilled by wells Eltmann,
338 Mürsbach 1 and 6 and Staffelstein 1 without reaching the underlying basement. Medium-amplitude
339 and semi-continuous reflections, characteristic of the Rotliegend in the study area, are also locally
340 observed, suggesting the presence of Rotliegend laterally away from wells (Fig. 7). Rotliegend units
341 are wedge shape and are tilted to the E-NE, onlapping to deep sited W-SW dipping normal faults in
342 the footwall of the Mürsbach and Lichtenfels reverse faults (Fig. 7). Interpreted W-SW dipping normal
343 faults appear to be crosscut by oppositely dipping (E-NE) Lichtenfels and Mürsbach reverse faults in
344 Buntsandstein units (Fig. 7). Clockwise E-NE block rotation in the hangingwall of these normal faults
345 created local half-grabens observed exclusively in the Rotliegend section (Fig. 7). In the hanging wall
346 of a normal fault located in the footwall of Lichtenfels Fault, the thickness of the Permian section is >
347 310 ms, TWT (ca. 580 m) thinning W-SW to ca. 85 ms, TWT (ca. 140 m) in the hangingwall of the
348 Mürsbach Fault (Fig. 7). The seismic interpretation of lateral thickness changes in the Permian is in
349 good accordance with 142.3 m minimum thickness of Permian drilled in well Mürsbach 6 (Table 1).
350 The thickness of the Permian section in the hanging wall of Bamberg Fault is > 200 ms, TWT (ca. 360
351 m) decreasing to the W-SW down to 3 m, drilled by well Eltmann (Fig. 7).

352 Sedimentary units in the hanging wall of Lichtenfels Fault are uplifted and gently folded where the
353 entire Jurassic and the upper parts of the Upper Triassic Keuper Group are eroded (Fig. 7). In the
354 footwall of Lichtenfels Fault sedimentary units are folded by a normal drag fold, creating a local
355 synform structure (also known as Hollfeld Syncline) where Jurassic rocks are preserved (Fig. 7). The
356 NW-SE striking Lichtenfels Fault is laterally and vertically segmented and is exposed at the surface over
357 ca. 16 km length (Fig. 1). In profile FRANKEN-1802, the Lichtenfels Fault has 135 ms TWT (ca. 230 m)
358 throw, measured at the top of the Buntsandstein (Fig. 7). The Mürsbach Fault strikes NNW-SSE over
359 ca. 5 km and it has been imaged by the Mürsbach seismic survey along three short (<4 km) 2D seismic
360 sections (Unpublished internal report 1967). The Mürsbach Fault shows ca. 65 ms TWT (ca. 100 m)
361 throw measured at the Buntsandstein top. Both, Muschelkalk and Keuper units are folded, creating a

https://doi.org/10.5194/se-2021-95
Preprint. Discussion started: 2 August 2021


Solid Earth
Discussions
Open Access
EGU

local anticline in the hangingwall of the Mürsbach Fault. Upper parts of the Keuper and younger units are eroded on the hangingwall side while in the immediate footwall some of the Jurassic units are still preserved (Fig. 7). E-NE dipping normal faults interpreted in the SW part of the profile FRANKEN-1802 are subparallel to the SE extension of the Kissingen-Haßfurt Fault Zone (Fig. 7).

At the well Eltmann location 94 m of ?Devonian metasedimentary rocks are drilled below the sedimentary cover and correlated with BSF1 (Fig. 7, (Trusheim, 1964). Identified BSF1 units are ca. 800 ms TWT (ca. 1400 m) thick in the NE of the seismic section, decreasing to 94 m towards the SW at the location of well Eltmann. BSF2 reflections show a concave up geometry below the Lichtenfels and Mürsbach faults and reach to the shallower depth towards the west (Fig. 7). In the center of the profile some high amplitude reflections of BSF2 branch off from the main reflection package and extend into the deeper parts of the crust (Fig. 7).

4.3 Profile FRANKEN-1803

This profile is subparallel to the profile FRANKEN-1801 and strikes NW-SE over 71.8 km length (Fig. 1). Well Obernsees is located 945 m SW of this profile and drilled into the 140 m of Jurassic, the entire Triassic succession and 55.7 m of Upper Permian Zechstein units (Table 1 and Fig. 8, (Gudden and Schmid, 1985). Jurassic units are preserved at the surface, except in the SE and NW parts of profile 1803, indicating a gentle synformal geometry with thickest parts of remnant Jurassic units in the center of the profile (Fig. 8). Triassic intervals show subparallel boundaries with only minor lateral thickness changes. At well Obernsees, the Rotliegend is only 18.3 m thick overlying metasedimentary rocks of possibly Late Paleozoic (Stettner and Salger, 1985; Ravidà et al., 2021). The reduced thickness of Rotliegend units in well Obernsees is related to a local basement high in the footwall of a E-SE dipping normal fault (Fig. 8). In the hanging wall of this normal fault and to its NW, medium amplitude and semi-continuous reflections below the top Zechstein horizon are interpreted as Rotliegend (Fig. 8, (Stettner and Salger, 1985; Schuh, 1985). Permian units are underlain by Paleozoic metasedimentary rocks and Variscan nappes (BSF1 units, Fig. 8). BSF2 reflections are sub-horizontal (between 2000-2500 ms, TWT) along the profile FRANKEN-1803 and gradually get shallower to the NW to reach to ca. 1200 ms TWT. From the SE to the center of the profile, BSF2 reflections become less reflective and appear to be segmented, into a steeper and a sub-horizontal segment (Fig. 8). Farther NW, BSF2 reflections reach to shallower depth and are also imaged by perpendicular FRANKEN-1802 and 1804 profiles. Lateral segmentation and changes in the reflectivity of the BSF2 might be related to the 3D geometry of an interpreted detachment/shear zone (Fig. 8).

4.4 Profile FRANKEN-1804

This profile strikes NE-SW over 63.3 km length, subparallel to the profile FRANKEN-1802 (Fig. 9). Jurassic units are preserved in the NE and the central part of the profile. To the SW however, Jurassic units are eroded and Keuper sandstones are exposed at the surface (Fig. 9). Geometries of Triassic units are fairly tabular, generally with shallow dips to the NE-E, but with variable dip angles between fault blocks. High amplitude and continuous reflections below the Triassic units are interpreted as Zechstein and are correlated with similar reflection packages in perpendicular profiles FRANKEN-1801 and 1803. Semi-continuous and medium amplitude reflections beneath the Zechstein are interpreted as Rotliegend that locally onlaps to the hanging wall of deep sited W-SW dipping normal faults (Fig. 9). In general, Permian units are wedge shaped in the hangingwalls of normal faults and are thinning laterally. Paleozoic metasedimentary units and Variscan nappes (BSF1) underlay the Permian and are ca. 1400 ms TWT (ca. 3000 m) thick in the center of the profile but thin laterally. Variscan shear zone (BSF2) underlying Paleozoic metasedimentary units and Variscan nappes are concave shaped in the NE and reach to shallower depth towards the SW edge of the profile FRANKEN-1804 (Fig. 9). In the

https://doi.org/10.5194/se-2021-95
Preprint. Discussion started: 2 August 2021


Solid Earth
Discussions
Open Access
EGU

center of the profile, BSF2 reflections are observed at greater depth up to about 3000 ms TWT and are slightly less reflective. Saxothuringian basement and possible lower parts of inner shelf facies (BSF3) characterize the deeper parts of the profile FRANKEN-1804 (Fig. 9).

At the NE edge of the profile FRANKEN-1804, the Eisfeld-Kulmbach Fault accumulates ca. 660 ms TWT (ca. 1300 m) of throw, exposing Buntsandstein in its hangingwall (Fig. 9). Across the fault, Jurassic units are preserved in the footwall and thin towards the SW where they are eroded in the hangingwall of the Asslitz Fault (Fig. 9). Asslitz fault accumulates ca. 180 ms TWT (ca. 390 m) of throw at the top of the Buntsandstein. Farther SW, the Lichtenfels Fault offsets Permian to Upper Triassic units with ca. 90 ms TWT (ca. 150 m) of throw measured at the Muschelkalk top. In contrast to profile FRANKEN-1802 located ca. 9 km NW, along the profile FRANKEN-1804 Lichtenfels Fault does not reach to the surface and dies out within the Keuper units. In the footwall of Lichtenfels Fault a W-SW dipping normal fault creates a local half-graben where continuous and medium amplitude reflections are onlapping and terminating against the fault (Fig. 9). Further SW, Bamberg Fault is a major normal fault displacing the Triassic and Permian units with ca. 25 ms TWT (ca. 45 m) offset measured at top Muschelkalk. Bamberg Fault detaches into the underlying Variscan shear zone (BSF2) at depth (Fig. 9). Farther north along the profile FRANKEN-1802, Bamberg fault is displaced by the Mürsbach reverse fault (Fig. 7).

5 Discussion

5.1 Westward extension of the Saxothuringian zone

Exposed Variscan allochthons are tectonically placed above the Paleozoic outer shelf facies (Bavarian facies) defined as fine grained and clay rich material preserved in the surrounding and below Variscan nappe piles (Linnemann and Heuse, 2001; Franke and Stein, 2000). BSF1 units observed beneath the sedimentary cover west of the FFS (Figs. 7 and 9) are interpreted as equivalents of Paleozoic metasedimentary rocks and Variscan nappe units (e.g. Münchberg nappe (Fig. 10). BSF1 units are mapped as far as ca. 65 km west of the FFS and are thinning towards the NW along the NW-SE striking profiles (Figs. 6 and 8) and towards the SW along the NE-SW (Figs. 7 and 9) striking profiles, showing a general westward thinning of Variscan nappes and Paleozoic metasedimentary rocks. Wells drilled in the Schwarzwald and Upper Rhein Graben areas (ca. 300 km SW of the study area) show low-grade metasedimentary units (shales and phyllites) and volcanic rocks below sedimentary cover, interpreted as SW extension of the Saxothuringian Zone (Franke et al., 2017). Although seismic reflection and few well data confirm the presence of low to very low-grade metasedimentary rocks below the Permian to Jurassic sedimentary cover in the study area, to date no well has probed the Variscan nappes west of the FFS. Seismic signatures of exposed Variscan nappes and low grade metasedimentary rocks east of the FFS do not allow differentiation between nappes and metasedimentary rocks. Similar observations have been made in the Caledonides of western Norway (Fazlikhani et al., 2017; Lenhart et al., 2019). Differentiation of Paleozoic inner and outer shelf facies is also beyond the resolution of available seismic reflection data. However, the tectonostratigraphic position of Variscan nappes and metasedimentary rocks relative to basal shear zones in exposed basement units east of the FFS (Heuse et al., 2010; Linnemann et al., 2010), highlights the possible presence of Variscan nappes and underlying inner and outer shelf facies ca. 65 km west of FFS (Fig. 10).

In the exposed parts of the Saxothuringian zone east of FFS, kinematic indicators show a top-to-the W-SW tectonic transport under NE-SW compression (Schwan, 1974). This deformation phase has been described as “D1” deformation phase before ca. 340 Ma, being related to the subduction and collision during the Variscan Orogeny (Kroner et al., 2007). For the assemblage of the Variscan during the subduction and collision a top-to-the NW tectonic transport under a NW-SE compression has also been proposed (Franke and Stein, 2000). Observed regional westward shallowing of mapped thrust

https://doi.org/10.5194/se-2021-95
Preprint. Discussion started: 2 August 2021

shear zones west of FFS could however been developed under both proposed tectonic transport directions.

5.2 Shear zone topography and strain localization during brittle deformation

A regional NW-SE dominated compressional/dextral transpressional phase during ca. 340-330 Ma affected the Saxothuringian zone and most likely reactivated preexisting D1 shear zones including the Münchberg Shear Zone, MSZ (Franke, 2000; Kroner et al., 2007). Assuming a rather initial flat geometry for the basal detachment/shear zone at the time of initiation, the 340-330 Ma deformation phase might also be responsible for the development of antiformal geometries observed along the mapped shear zone modifying the geometry of the D1 shear zone by folding and bending (Figs. 7 and 9). Alternatively, the antiformal geometry of the basal detachment/shear zone could be initiated during the latest Carboniferous-Early Permian due to the normal fault development. In the latter case shear zones appear to be rotated and uplifted (together with entire footwall block) on the footwall side of normal faults; creating an antiformal shape of shear zones (Figs. 7 and 9). Although the majority of brittle faults are developed on top of the antiformal parts of the basal detachment/shear zone, Lichtenfels Fault and the buried normal fault in its footwall are developed on top of the rather flat geometry of the basal detachment/shear zone (Fig. 9). This observation rather negates the scenario at which the development of Latest-Carboniferous - Permian normal faults is responsible mechanism for the modification of shear zone geometry. Hence, we interpret that the basal detachment/shear zone is folded due to latest Variscan tectonic events prior to the development of normal faults.

Some of the Latest-Carboniferous - Permian normal faults detach into the shear zones at depth, and potentially reactivate parts of the shear zone on their hangingwall side (Figs. 6-9). Comparable brittle reactivation of orogenic shear zones during initiation and activity of post-orogenic brittle faults has been described from the post-Caledonides (Fazlikhani et al., 2017; Phillips et al., 2016; Koehl et al., 2018; Wiest et al., 2020) and post-Variscan of the western Alps (Festa et al., 2020; Ballèvre et al., 2018). Initiated topography of the shear zones, most likely created during latest Variscan compressional tectonics, perturbs the regional stress field and localize the strain, facilitating initiation of normal and thrust faults. All the major reverse faults (e.g. Eisfeld-Kulmbach, Asslitz, Lichtenfels (northern portion) and Mürsbach faults) detach into the shear zone where the shear zone shows an antiformal geometry. At the location of FRANKEN-1804 (Fig. 9), in the footwall of the Bamberg normal fault, the underlying shear zone does not show antiformal geometry and no reverse fault has been developed, while ca. 10 km farther north along profile FRANKEN-1802 where the shear zone has an antiformal geometry Mürsbach reverse fault has been developed in the footwall of Bamberg fault (or another normal fault, Fig. 7). Presence or absence of antiformal geometry of basal detachment/shear zone appears to influence the amount of upper crustal brittle deformation (normal and reverse faults), showing the regional stress field perturbation and strain localization facilitating brittle fault development. This observation highlights the importance of preexisting shear zones geometry during brittle fault development in vertical section.

Presence or absence of antiformal geometry of the shear zone also appears to influence the amount of fault offset in the study area. In the NE of the profile FRANKEN-1802 where the Variscan shear zone developed antiformal geometry, Lichtenfels Fault shows ca. 180 ms TWT of throw at the top Muschelkalk horizon and is exposed at the surface. Along the profile FRANKEN-1804, ca. 10 km farther south, where the Variscan shear zone shows a rather flat geometry, Lichtenfels Fault has only ca. 80 ms TWT of throw and is a blind fault tipping out in the Keuper units. In addition, at the location of these antiformal parts of the shear zone a generally higher amount of upper crustal brittle deformation (normal and reverse faults) occurs, reflecting rather local fault concentration above the antiformal parts of the underlying shear zone. It should be noted that towards the E, at the margin of the Franconian Basin, FFS as the major basin bounding fault system displaces the basal

https://doi.org/10.5194/se-2021-95
Preprint. Discussion started: 2 August 2021

detachment/shear zone, exposing Variscan basement units on the hangingwall side. Comparing reverse faults with few hundred meters of offset detaching into the shear zones with the FFS having ca. 3 km of offset (Wagner et al., 1997) displacing the shear zone, shows that the amount of fault offset is an important controlling factor in reactivation or displacement of the shear zone by brittle faults. The amount of fault offset together with the previously shown mechanical/rheological properties of shear zones and their map view orientation relative to the extensional/shortening direction are thus important controlling factors in reactivation or displacement of the basal detachment/shear zone by brittle faults (Heilman et al., 2019; Fazlikhani et al., 2021; Phillips et al., 2019; Fazlikhani et al., 2017; Daly et al., 1989; Ring, 1994).

5.3 Post Variscan Rotliegend basins in SE Germany and their regional context

Latest stages of Variscan tectonics and post orogenic thermal relaxation during Late Carboniferous and Early Permian is marked by the development of intermontane basins in the internal parts of the Variscan belt (Arthaud and Matte, 1977; McCann et al., 2006). These intermontane basins are mainly located in the hangingwall of normal faults in graben and half-graben settings and therefore are relatively small (km to tens of km), deep and isolated basins accumulating continental clastic sediments with rapid lateral thickness changes (McCann et al., 2006). Fault bounded Rotliegend basins in SE Germany are interpreted to have developed in an extensional and/or transtensional setting during the latest Carboniferous and Permian time as evidenced by rather abrupt lateral thickness and sedimentary facies changes (Schröder, 1988, 1987; Peterek et al., 1996c; Leitz and Schröder, 1985; Arthaud and Matte, 1977; Dill, 1988; Müller, 1994; Peterek et al., 1997; McCann et al., 2006; Helmkampf et al., 1982). Rotliegend sedimentary rocks in the study area are exposed in the footwall and hangingwall of the FFS from NW to SE in the Stockheim, Rugendorf, Wirsberg and Weidenberg outcrops (Fig. 1). Well Wolfersdorf (Stockheim outcrop) drilled 726 m of Rotliegend, while the upper parts of the section are eroded, suggesting that originally even thicker Rotliegend sections (ca. 1000 m) were deposited (Herrmann, 1958; Dill, 1988; Paul and Schröder, 2012). About 18 km west of well Wolfersdorf, well Mittelberg drilled only 41 m of Rotliegend before reaching basement rocks (Friedlein and Hahn, 2018). Similar rapid thickness changes of the Rotliegend units were also observed in the Weidenberg, Erbendorf, Weiden and Schmidgaden areas, all originally interpreted as small, isolated fault-bounded basins, but now, interpreted as individual exposures of one coherent depositional area, the NW-SE Naab Basin, where the Rotliegend reaches up to 2800 m thickness (Paul and Schröder, 2012). The Naab Basin is bordered by normal faults, some of which reactivated as reverse faults or are cross cut by younger reverse faults (Müller, 1994; Peterek et al., 1996b).

In addition to exposures along the FFS, several wells in the western parts of the study area (e.g. Staffelstein 1, Mürsbach 1 & 6, and Eltmann) also encountered Rotliegend that relates to the SW-NE Kraichgau Basin (Table 1, Fig. 1) of which the NW-SE Naab Basin is considered as a basin compartment (Paul, 2006). Among these wells, only Eltmann and Mittelberg reached the Rotliegend base showing a general westward thinning of Rotliegend units from the FFS (Table 1). This corresponds to the pattern of isopach maps, showing a gradual thickening of Rotliegend units to reach maximum thicknesses of ca. 2000 m in the easternmost parts of the Kraichgau Basin (Sitting and Nitsch, 2012).

Rotliegend basin architecture in the Variscan Internides, with the Saar-Nahe, Kraichgau and Schramberg basins as prominent examples, is characterized by 10-100 km wide and long basins bordered by normal faults, rather related to the extensional forces than the collapse of overthickened crust during the orogeny (Henk, 1997). In comparison, post-Caledonian Devonian basins in western Norway developed as supra-detachment basins that are bounded by brittle normal faults reactivating

https://doi.org/10.5194/se-2021-95
Preprint. Discussion started: 2 August 2021

pre-existing Caledonian thrusts (Fossen, 2010; Fazlikhani et al., 2017; Wiest et al., 2020; Lenhart et al., 2019; Séranne and Séguret, 1987; Osmundsen and Andersen, 2001). Post-Caledonian supradetachment basins in western Norway accumulate >26 km of Devonian units that is almost three times more than the true depth of the basin (Vetti and Fossen, 2012; Séranne and Séguret, 1987). In the northern North Sea and its western margin onshore Scotland and Shetland, and offshore East Shetland Platform, post-Caledonian Devonian basins are interpreted as normal fault bounded half-graben basins that in some cases detach onto Caledonian thrust/shear zones (Coward et al., 1989; Platt and Cartwright, 1998; Fazlikhani et al., 2017; Norton et al., 1987; Séranne, 1992; Patruno et al., 2019; Phillips et al., 2019; Fazlikhani et al., 2021).

Range of post-orogenic basin architecture observed in Caledonian and Variscan orogenies highlights the importance of preexisting orogenic thrust/shear zones. Comparison of post-Caledonian basins with post-Variscan basins show that in the Caledonian cases pre-existing detachment/shear zone play more important role in basin development and architecture than in the post-Variscan basins, observed in the study area. Normal faults bounding post-Variscan basins appear not to reactivate entire Variscan thrust/shear zones except for the Saar-Nahe Basin (Henk, 1993). Observed variations in post-orogenic basin architecture might be related to the differences in the exposed level of the basement. Exposed Devonian basin of western Norway show deeper levels of crust in compare to Devonian basins in the western margin of North Sea rift. It should be noted that the post-orogenic extension direction relative to the orientation of the orogenic structures in addition to the amount and duration of the post-orogenic extension might also influence basin architecture.

5.4 Brittle fault development and relative age relationships

Post-Variscan extensional phases resulted in the development of normal faults bounding Rotliegend half-graben and graben basins observed across the Variscan belt (Peterek et al., 1997; Arthaud and Matte, 1977; McCann et al., 2006; Schröder, 1987; Müller, 1994; Stephenson et al., 2003). Mapped seismic scale normal faults in the study area can be divided into three main groups, based on their stratigraphic position: I) normal faults developed at shallower depth which terminate in the lower Triassic or Upper Permian (Zechstein) intervals (Figs. 6-9). II) normal faults developed in the deeper parts of the stratigraphy displacing Permian units and continuing into the pre-Permian units with their upper tip terminating in Uppermost Permian (Zechstein) or Lowermost Triassic units (e.g. normal faults in the footwall of Lichtenfels and Asslitz reverse faults, Figs. 6-9). III) small groups of normal faults which displace the entire stratigraphy and die out into the pre-Permian units (Figs. 6 and 9). The first group of normal faults which developed in the Triassic unit only, do not show synsedimentary activity detectable in seismic profiles and are interpreted to most likely originate from sedimentary loading and differential compaction during a regional tectonic quiescence in Triassic and Jurassic times (Peterek et al., 1997; Fazlikhani et al., 2021; Fazlikhani and Back, 2015). The second group of normal faults, displacing mainly the Permian succession, is interpreted to have developed during post-orogenic extension in latest Carboniferous-Permian (Stephanian/Rotliegend) time. This second group of normal faults shows widespread evidence of synsedimentary activity and is bounding Permian half graben and graben basins (buried and exposed) in southern Germany. In the majority of cases the first and second group of normal faults are not vertically linked. This observation can be explained by the presence of fine grained marine and in some places evaporitic Zechstein units, acting as a semi-ductile/ductile layer accommodating strain. However, in few instances the Zechstein, together with Triassic units are displaced by the third group of normal faults (Figs 6 and 9). It should be noted that with the available dataset it is not clear whether the third group of normal faults is the result of an upsection growth of Permian faults, downsection growth of the Triassic-Jurassic faults or whether they developed due to the downsection growth of Triassic –Jurassic faults linking to and reactivating preexisting Permian faults.

https://doi.org/10.5194/se-2021-95
Preprint. Discussion started: 2 August 2021

In addition to normal faults, the major km-long NW-SE striking Eisfeld-Kulmbach, Asslitz, Lichtenfels and Mürsbach reverse faults are located west of the FFS, displacing and folding the Permian to Jurassic sedimentary cover. Reverse faults are better developed in the eastern part of the study area and on top of the antiformal parts of the Variscan shear zones while towards the west, normal faults are dominating. Observed reverse faults are developed mainly in the footwalls of Permian normal faults and dip to the E-NE (Figs. 6-9). Reverse faults cut through the upper portion of Permian normal faults, translating Permo-Mesozoic units to the W-SW. Farther north of the study area in the Thuringian Basin and northern Germany, similar reverse faults are related to the Cretaceous inversion event (Kley and Voigt, 2008; Navabpour et al., 2017). Therefore, it appears that the youngest generation of seismic-scale brittle faults are the reverse faults. However, whether reverse faults only initiated during the Cretaceous inversion and younger events or rather are reverse reactivated east dipping Permian normal faults is still unclear and needs further investigation.

6 Conclusion

In this study we combine existing 2D seismic reflection profiles, well data and surface geological information to interpret the recently acquired 2D FRANKEN seismic survey in SE Germany. Three Basement Seismic Facies (BSF1-3) are described below the Permian-Mesozoic sedimentary cover that are interpreted as Variscan units and structures. We investigate possible westward continuation of Variscan units and structures and discuss the influence of Variscan structures in latest to post-Variscan basin development. We show that:

- Variscan units and structures extend to ~65 km west of the FFS that are covered by sedimentary rocks of the Kraichgau/Franconian Basin.
- Low-grade metasedimentary rocks and possible nappe units (BSF1) in the hanging wall of Variscan shear zones are wedge shaped and thin out towards the W-SW.
- Variscan relative autochthons occupy footwall of shear zones.
- Shear zones show local syn- and antiformal geometries and reach to the base of Permian-Mesozoic sedimentary cover towards the W-SW.
- Geometry of shear zones control the location at which major Permian normal faults have developed.
- Permian normal faults dip to various orientations, creating Rotliegend graben and half-graben basins. Observed Rotliegend half-graben basins in the east are interpreted as the NW continuation of the Naab Basin. Towards the west, observed Rotliegends are associated to the Kraichgau Basin.
- Thickness of Triassic sedimentary rocks is fairly constant, highlighting a regional tectonic quiescence in the study area.
- Some of the Permian normal faults are cross cut by oppositely dipping reverse faults most likely during the regional Cretaceous inversion event occurred in Central Europe. Reverse faults are interpreted as reactivated preexisting Permian normal faults.
- Reactivated normal faults are located to the eastern parts of the study area where preexisting Variscan shear zone show syn and antiformal geometry

We document westward continuation of Variscan shear zones away from the Bohemian Massif for the first time and show how the geometry of shear zones localize the strain and influence the development of latest to post-orogenic faults and basins.

https://doi.org/10.5194/se-2021-95
Preprint. Discussion started: 2 August 2021

638 **Data availability**

639 DEKORP seismic data are available via GFZ (Deutsche GeoForschungsZentrum) Potsdam. Utilized well
640 data can be access through the Geological Survey of Bavaria (Bayerisches Landesamt für Umwelt -
641 LfU). FRANKEN seismic data are acquired for the ongoing Geothermal Alliance Bavaria (GAB) research
642 project and are not publically available yet.

643

644 **Author contributions**

645 HF integrated utilized datasets, interpreted seismic reflection and prepared the manuscript. WB and
646 HS acquired the financial support and contributed to the reviewing, improvement and the discussion
647 of the presented results.

648

649 **Competing interests**

650 The authors declare that they have no conflict of interest.

651

652 **Acknowledgment**

653 This contribution is part of the Geothermal Alliance Bavaria (GAB) project funded by the Bavarian State
654 Ministry of Education and Cultural Affairs, Science and Art to the Friedrich-Alexander-University
655 Erlangen-Nuremberg (FAU), The Technical University of Munich (TUM) and the University of Bayreuth.
656 We would like to thank the Bayerisches Landesamt für Umwelt (LfU) for providing well data and fruitful
657 discussions. Schlumberger is thanked for providing academic licenses for Petrel and supporting the 3D
658 subsurface Lab at the Friedrich-Alexander-University Erlangen-Nuremberg. All authors would like to
659 thank the members of the GAB project for the discussions increasing the quality of this contribution.

660

661 References

662 Arthaud, F. and Matte, P.: Late Paleozoic strike-slip faulting in southern Europe and northern Africa:
663 Result of a right-lateral shear zone between the Appalachians and the Urals, GSA Bulletin, 88,
664 1305–1320, https://doi.org/10.1130/0016-7606(1977)88<1305:LPSFIS>2.0.CO;2, 1977.
665 Bader, K. and Bram, K. (Eds.): Der mittelfränkische Gebirgsrücken südlich Nürnberg, Schweizerbart
666 Science Publishers, Stuttgart, Germany, 2001.
667 Ballèvre, M., Manzotti, P., and Dal Piaz, G. V.: Pre-Alpine (Variscan) Inheritance: A Key for the
668 Location of the Future Valaisan Basin (Western Alps), Tectonics, 37, 786–817,
669 https://doi.org/10.1002/2017TC004633, 2018.
670 Behr, H. J. and Heinrichs, T.: Geological interpretation of DEKORP 2-S: A deep seismic reflection
671 profile across the Saxothuringian and possible implications for the Late Variscan structural
672 evolution of Central Europe, Tectonophysics, 142, 173–202, https://doi.org/10.1016/0040-
673 1951(87)90122-3, available at:
674 https://www.sciencedirect.com/science/article/pii/0040195187901223, 1987.

https://doi.org/10.5194/se-2021-95
Preprint. Discussion started: 2 August 2021

675 Bergerat, F. and Geyssant, J.: Tectonique cassante et champ de contraintes tertiaire en avant des
676 Alpes orientales: le Jura souabe, Geologische Rundschau, 71, 537–548, 1982.
677 Boy, J. A., Haneke, J., Kowalczyk, G., Lorenz, V., Schindler, T., Stollhofen, H., and Thum, H.: Rotliegend
678 im Saar-Nahe-Becken, am Taunus-Südrand und im nördlichen Oberrheingraben, in:
679 Innervariscische Becken, edited by: Lützner, H., Schweizerbart Science Publishers, Stuttgart,
680 Germany, 254–377, 2012.
681 Buness, H.-A. and Bram, K.: Die Muschelkalkoberfläche und die permische Peneplam in
682 Mittelfranken abgeleitet aus seismischen Messungen, in: Der mittelfränkische Gebirgsrücken
683 südlich Nürnberg, edited by: Bader, K. and Bram, K., Schweizerbart Science Publishers, Stuttgart,
684 Germany, 35–59, 2001.
685 Carlé, W.: Bau und Entwicklung der Südwestdeutschen Großscholle, Beihefte zum Geologischen
686 Jahrbuch, 1955.
687 Cassinis, G., Toutin-Morin, N., and Virgili, C.: A General Outline of the Permian Continental Basins in
688 Southwestern Europe, in: The Permian of Northern Pangea.: Volume 2: Sedimentary Basins and
689 Economic Resources, edited by: Scholle, P., Peryt, t. M., and Ulmer-Scholle, D. S., Springer, Berlin,
690 137–157, 1995.
691 Chateauneuf, J. J. and Farjanel, G.: Synthèse Géologique des Bassins Permiens Français, 128th ed.,
692 1989.
693 Collanega, L., Siuda, K., A.-L. Jackson, C., Bell, R. E., Coleman, A. J., Lenhart, A., Magee, C., and Breda,
694 A.: Normal fault growth influenced by basement fabrics: The importance of preferential
695 nucleation from pre-existing structures, Basin Res, 31, 659–687,
696 https://doi.org/10.1111/bre.12327, 2019.
697 Coubal, M., Málek, J., Adamovič, J., and Štěpančíková, P.: Late Cretaceous and Cenozoic dynamics of
698 the Bohemian Massif inferred from the paleostress history of the Lusatian Fault Belt, Journal of
699 Geodynamics, 87, 26–49, https://doi.org/10.1016/j.jog.2015.02.006, 2015.
700 Coward, M. P., Enfield, M. A., and Fischer, M. W.: Devonian basins of Northern Scotland: extension
701 and inversion related to Late Caledonian — Variscan tectonics, Geological Society, London,
702 Special Publications, 44, 275, https://doi.org/10.1144/GSL.SP.1989.044.01.16, 1989.
703 Daly, M. C., Chorowicz, J., and Fairhead, J. D.: Rift basin evolution in Africa: the influence of
704 reactivated steep basement shear zones, Geological Society, London, Special Publications, 44,
705 309–334, https://doi.org/10.1144/GSL.SP.1989.044.01.17, 1989.
706 DEKORP and Orogenic Processes Working Group: Structure of the Saxonian Granulites: Geological
707 and geophysical constraints on the exhumation of high-pressure/high-temperature rocks in the
708 mid-European Variscan belt, Tectonics, 18, 756–773, https://doi.org/10.1029/1999TC900030,
709 1999.
710 DEKORP Research Group: Crustal structure of the Saxothuringian Zone: Results of the deep seismic
711 profile MVE-90(East), Zeitschrift für Geologische Wissenschaften, 22, 647–769, available at:
712 http://www.zgw-online.de/en/, 1994a.
713 DEKORP Research Group: DEKORP 3/MVE 90(West) - preliminary geological interpretation of a deep
714 near-vertical reflection profile between the Rhenish and Bohemian Massifs, Germany, Zeitschrift
715 für Geologische Wissenschaften, 22, 771–801, 1994b.
716 Dill, H.: Sedimentpetrographie des Stockheimer Rotliegendbeckens, Nordostbayern, Schweizerbart
717 Science Publishers, Stuttgart, Germany, 1988.
718 Edel, J. B. and Weber, K.: Cadomian terranes, wrench faulting and thrusting in the central Europe
719 Variscides: geophysical and geological evidence, Geologische Rundschau, 84, 412–432,
720 https://doi.org/10.1007/BF00260450, 1995.
721 Ehling, B.-C. and Gebhardt, U.: Rotliegend im Saale-Becken, in: Innervariscische Becken, edited by:
722 Lützner, H., Schweizerbart Science Publishers, Stuttgart, Germany, 504–516, 2012.

https://doi.org/10.5194/se-2021-95
Preprint. Discussion started: 2 August 2021

723 Emmert, U., Gudden, H., Haunschild, H., Meyer, R. K. F., Schmid, H., Schuh, H., and Stettner, G.:
724 Bohrgut-Beschreibung der Forschungsbohrung Obernsees, Geologica Bavarica, 88, 23–47, 1985.
725 Engel, W., Feist, R., and Franke, W.: Le Carbonifère anté-Stéphanien de la Montagne Noire: rapports
726 entre mise en place des nappes et sédimentation., Bulletin du BRGM, 1, 341–389, 1982.
727 Eynatten, H. von, Kley, J., Dunkl, I., Hoffmann, V.-E., and Simon, A.: Late Cretaceous to Paleogene
728 exhumation in central Europe – localized inversion vs. large-scale domal uplift, Solid Earth, 12,
729 935–958, https://doi.org/10.5194/se-12-935-2021, available at:
730 https://se.copernicus.org/articles/12/935/2021/, 2021.
731 Fazlikhani, H. and Back, S.: The influence of differential sedimentary loading and compaction on the
732 development of a deltaic rollover, Marine and Petroleum Geology, 59, 136–149,
733 https://doi.org/10.1016/j.marpetgeo.2014.08.005, 2015.
734 Fazlikhani, H., Aagotnes, S. S., Refvem, M. A., Hamilton-Wright, J., Bell, R. E., Fossen, H., Gawthorpe,
735 R. L., Jackson, C. A.-L., and Rotevatn, A.: Strain migration during multiphase extension, Stord
736 Basin, northern North Sea rift, Basin Res, 33, 1474–1496, https://doi.org/10.1111/bre.12522,
737 2021.
738 Fazlikhani, H., Fossen, H., Gawthorpe, R. L., Faleide, J. I., and Bell, R. E.: Basement structure and its
739 influence on the structural configuration of the northern North Sea rift, Tectonics, 36, 1151–
740 1177, https://doi.org/10.1002/2017TC004514, 2017.
741 Festa, A., Balestro, G., Borghi, A., Caroli, S. de, and Succo, A.: The role of structural inheritance in
742 continental break-up and exhumation of Alpine Tethyan mantle (Canavese Zone, Western Alps),
743 Geoscience Frontiers, 11, 167–188, https://doi.org/10.1016/j.gsf.2018.11.007, available at:
744 http://www.sciencedirect.com/science/article/pii/S1674987118302470, 2020.
745 Fossen, H.: Extensional tectonics in the North Atlantic Caledonides: a regional view, Geological
746 Society, London, Special Publications, 335, 767, https://doi.org/10.1144/SP335.31, 2010.
747 Franke, W.: The mid-European segment of the Variscides: tectonostratigraphic units, terrane
748 boundaries and plate tectonic evolution, in: Orogenic Processes: Quantification and Modelling in
749 the Variscan Belt, edited by: Franke, W., Haak, V., Oncken, O., and Tanner, D. C., 35,
750 https://doi.org/10.1144/GSL.SP.2000.179.01.05, 2000.
751 Franke, W. and Stein, E.: Exhumation of high-grade rocks in the Saxo-Thuringian Belt: Geological
752 constraints and geodynamic concepts, in: Orogenic Processes: Quantification and Modelling in
753 the Variscan Belt, https://doi.org/10.1144/GSL.SP.2000.179.01.20, 2000.
754 Franke, W., Behrmann, J., and Moehrmann, H.: Zur Deformationsgeschichte des Kristallins im
755 Münchberger Deckenstapel, KTB Report, 92-4, 225–240, 1992.
756 Franke, W.: Tectonostratigraphic units in the Variscan belt of central Europe, in: Terranes in the
757 Circum-Atlantic Paleozoic Orogens, edited by: Dallmeyer, R. D., Geological Society of America, 0,
758 https://doi.org/10.1130/SPE230-p67, 1989.
759 Franke, W., Cocks, L. R. M., and Torsvik, T. H.: The Palaeozoic Variscan oceans revisited, Gondwana
760 Research, 48, 257–284, https://doi.org/10.1016/j.gr.2017.03.005, 2017.
761 Franke, W., Haak, V., Oncken, O., and Tanner, D. C. (Eds.): Orogenic Processes: Quantification and
762 Modelling in the Variscan Belt, 179, 2000.
763 Franz, M., Nowak, K., Berner, U., Heunisch, C., Bandel, K., Röhling, H.-G., and Wolfgramm, M.:
764 Eustatic control on epicontinental basins: The example of the Stuttgart Formation in the Central
765 European Basin (Middle Keuper, Late Triassic), Global and Planetary Change, 122, 305–329,
766 https://doi.org/10.1016/j.gloplacha.2014.07.010, available at:
767 https://www.sciencedirect.com/science/article/pii/S092181811400143X, 2014.
768 Freudenberger, W. and Schwerd, K.: Erläuterungen zur Geologischen Karte von Bayern 1. Geol.
769 :500000, Bayerisches Geologisches Landesamt, München, 1996.

https://doi.org/10.5194/se-2021-95
Preprint. Discussion started: 2 August 2021

770 Freudenberger, W., Herold, B., and Wagner, S.: Bohrkern-Beschreibung und Stratigraphie der
771 Forschungsbohrungen Lindau 1 und Spitzeichen 1, Geologica Bavarica, 109, 15–26, 2006.
772 Freyberg, B. von: Tektonische Karte der Fränkischen Alb und ihrer Umgebung, Erlanger Geologische
773 Abhandlungen, 77, 1–81, 1969.
774 Friedlein, V. and Hahn, T.: Mittelberg well description: Internal report, Bayerisches Landesamt fuer
775 Umwelt, 2018.
776 Gudden, H.: Der Untere Keuper in Bohrungen zwischen Eltmann und Rodach, Geologische Blätter
777 von Nordost-Bayern, 31, 448–462, 1981.
778 Gudden, H.: Die Thermal-Mineralwasser-Erschließungsbohrung Staffelstein 1975, Brunnenbau, Bau
779 von Wasserwerken und Rohrleitungsbau (bbr), 28, 85–92, 1977.
780 Gudden, H. and Schmid, H.: Die Forschungsbohrung Obernsees—Konzeption, Durchführung und
781 Untersuchung der Metallführung, Geologica Bavarica, 88, 5–21, 1985.
782 Gudden, H.: Der Buntsandstein in der Forschungsbohrung Obernsees, Geologica Bavarica, 88, 69–81,
783 1985.
784 Gudden, H.: über die Struktur Mürsbach und ihre Eignung für behälterlose unterirdische
785 Gasspeicherung, München, 1971.
786 Gümbel, C. W. von: Geognostische Beschreibung des Königreichs Bayern. Dritte Abtheilung.
787 Geognostische Beschreibung des Fichtelgebirges mit dem Frankenwalde und dem westlichen
788 Vorlande., Perthes, Gotha, 1879.
789 Hahn, T., Kroner, U., and Mezer, P.: Lower Carboniferous synorogenic sedimentation in the Saxo-
790 Thuringian Basin and the adjacent Allochthonous Domain, in: Pre-Mesozoic geology of Saxo-
791 Thuringia: From the Cadomian active margin to the Variscan orogen, edited by: Linnemann, U.
792 and Romer, R. L., Schweizerbart, Stuttgart, 171–192, 2010.
793 Haunschild, H.: Der Keuper in der Forschungsbohrung Obernsees, Geologica Bavarica, 88, 103–130,
794 available at: https://www.lfu.bayern.de/geologie/geo_karten_schriften/schriften/index.htm,
795 1985.
796 Heilman, E., Kolawole, F., Atekwana, E. A., and Mayle, M.: Controls of Basement Fabric on the
797 Linkage of Rift Segments, Tectonics, 38, 1337–1366, https://doi.org/10.1029/2018TC005362,
798 2019.
799 Helmkampf, K. E.: Profilvergleich und sedimentologische Entwicklung im Umkreis der
800 Forschungsbohrungen Spitzeichen 1 und Lindau 1, Geologica Bavarica, 109, 63–94, 2006.
801 Helmkampf, K. E., Kuhlmann, J., and Kaiser, D.: Das Rotliegende im Bereich der Weidener Bucht, in:
802 Geologica Bavarica 83: Neue Tiefbohrungen in Bayern, edited by: Bayerisches Geologisches
803 Landesamt, Bayerisches Geologisches Landesamt, München, 167–186, 1982.
804 Henk, A.: Gravitational orogenic collapse vs plate-boundary stresses: a numerical modelling
805 approach to the Permo-Carboniferous evolution of Central Europe, Geologische Rundschau, 86,
806 39–55, https://doi.org/10.1007/s005310050120, 1997.
807 Henk, A.: Late orogenic Basin evolution in the Variscan internides: the Saar-Nahe Basin, southwest
808 Germany, Tectonophysics, 223, 273–290, https://doi.org/10.1016/0040-1951(93)90141-6,
809 available at: https://www.sciencedirect.com/science/article/pii/0040195193901416, 1993.
810 Herrmann, R.: Die stratigraphichen und tektonischen Verhältnisse des Stockheimer Beckens.,
811 Geologie, 7, 133–157, 1958.
812 Heuse, T., Blumenstengel, H., Elicki, O., Geyer, G., Hansch, W., Maletz, J., Sarmiento, G. N., and
813 Weyer, D.: Biostratigraphy - The faunal province of the southern margin of the Rheic Ocean, in:
814 Pre-Mesozoic geology of Saxo-Thuringia: From the Cadomian active margin to the Variscan
815 orogen, edited by: Linnemann, U. and Romer, R. L., Schweizerbart, Stuttgart, 99–170, 2010.

https://doi.org/10.5194/se-2021-95
Preprint. Discussion started: 2 August 2021

816 Kley, J. and Voigt, T.: Late Cretaceous intraplate thrusting in central Europe: Effect of Africa-Iberia-
817 Europe convergence, not Alpine collision, Geology, 36, 839–842,
818 https://doi.org/10.1130/G24930A.1, 2008.
819 Koehl, J.-B. P., Bergh, S. G., Henningsen, T., and Faleide, J. I.: Middle to Late Devonian–Carboniferous
820 collapse basins on the Finnmark Platform and in the southwesternmost Nordkapp basin, SW
821 Barents Sea, Solid Earth, 9, 341–372, https://doi.org/10.5194/se-9-341-2018, available at:
822 https://www.solid-earth.net/9/341/2018/, 2018.
823 Kossmat, F.: Gliederung des varistischen Gebirgsbaues., Abhandlungen des Sächsischen
824 Geologischen Landesamtes, 1, 1–39, 1927.
825 Krohe, A.: Variscan tectonics of central Europe: Postaccretionary intraplate deformation of weak
826 continental lithosphere, Tectonics, 15, 1364–1388, https://doi.org/10.1029/96TC01110,
827 available at: https://www.scopus.com/inward/record.uri?eid=2-s2.0-
828 0030390295&doi=10.1029%2f96TC01110&partnerID=40&md5=a69bf89c67177c6a9a7d76d35a9
829 3aee5, 1996.
830 Kroner, U., Hahn, T., Romer, R. L., and Linnemann, U.: The Variscan orogeny in the Saxo-Thuringian
831 zone—Heterogenous overprint of Cadomian/Paleozoic Peri-Gondwana crust, in: The Evolution of
832 the Rheic Ocean: From Avalonian-Cadomian Active Margin to Alleghenian-Variscan Collision,
833 edited by: Linnemann, U., Nance, R. D., Kraft, P., and Zulauf, G., Geological Society of America,
834 119, https://doi.org/10.1130/2007.2423(06), 2007.
835 Kroner, U. and Goerz, I.: Variscan assembling of the Allochthonous Domain of the Saxo-Thuringian
836 Zone - a tectonic model, in: Pre-Mesozoic geology of Saxo-Thuringia: From the Cadomian active
837 margin to the Variscan orogen, edited by: Linnemann, U. and Romer, R. L., Schweizerbart,
838 Stuttgart, 271–286, 2010.
839 Laversanne, J.: Le Permian de Lodeve (Massif Central Francais). Evolution des depots Autuniens et
840 exemples de mineralisations uraniferes diagenetiques par circulation de solutions exogenes,
841 1978.
842 Leitz, F. and Schröder, B.: Die Randfazies der Trias und Bruchschollenland südöstlich Bayreuth
843 (Exkursion C am 11. und 12. April 1985), Jahresberichte und Mitteilungen des Oberrheinischen
844 Geologischen Vereins, 67, 51–63, https://doi.org/10.1127/jmogv/67/1985/51, 1985.
845 Lenhart, A., Jackson, C. A.-L., Bell, R. E., Duffy, O. B., Gawthorpe, R. L., and Fossen, H.: Structural
846 architecture and composition of crystalline basement offshore west Norway, Lithosphere, 11,
847 273–293, https://doi.org/10.1130/L668.1, 2019.
848 Linnemann, U. and Romer, R. L. (Eds.): Pre-Mesozoic geology of Saxo-Thuringia: From the Cadomian
849 active margin to the Variscan orogen, Schweizerbart, Stuttgart, 488 pp., 2010.
850 Linnemann, U. and Heuse, T.: The Ordovician of the Schwarzburg Anticline: Geotectonic setting,
851 biostratigraphy and sequence stratigraphy (Saxo-Thuringian Terrane, Germany), Zeitschrift der
852 Deutschen Geologischen Gesellschaft, 151, 471–491,
853 https://doi.org/10.1127/zdgg/151/2001/471, 2001.
854 Linnemann, U., Hofmann, M., Romer, R. L., and Gerdes, A.: Transitional stages between the
855 Cadomian and Variscan orogenies: Basin development and tectono-magmatic evolution of the
856 southern margin of the Rheic Ocean in the Saxo-Thuringian Zone (North Gondwana shelf), in:
857 Pre-Mesozoic geology of Saxo-Thuringia: From the Cadomian active margin to the Variscan
858 orogen, edited by: Linnemann, U. and Romer, R. L., Schweizerbart, Stuttgart, 59–98, 2010.
859 Lüschen, E., Wenzel, F., Sandmeier, K.-J., Menges, D., Rühl, T., Stiller, M., Janoth, W., Keller, F.,
860 Söllner, W., Thomas, R., Krohe, A., Stenger, R., Fuchs, K., Wilhelm, H., and Eisbacher, G.: Near-
861 vertical and wide-angle seismic surveys in the Black Forest, SW Germany, Journal of Geophysics,
862 62, 1–30, 1987.

https://doi.org/10.5194/se-2021-95
Preprint. Discussion started: 2 August 2021

863 Lützner, H., Andreas, D., Schneider, J. W., Voigt, S., and Werneburg, R.: Stefan und Rotliegend im
864 Türinger Wald und seiner Umgebung, in: Innervariscische Becken, edited by: Lützner, H.,
865 Schweizerbart Science Publishers, Stuttgart, Germany, 418–487, 2012.
866 Matter, A., Peters, T. J., Bläsi, H. R., and and Ziegler, H. J.: Sondierbohrung Riniken, in: NAGRA
867 Technischer Bericht, 1–214, 1987.
868 McCann, T., Pascal, C., Timmerman, M. J., Krzywiec, P., López-Gómez, J., Wetzel, L., Krawczyk, C. M.,
869 Rieke, H., and Lamarche, J.: Post-Variscan (end Carboniferous-Early Permian) basin evolution in
870 Western and Central Europe, Geological Society, London, Memoirs, 32, 355–388,
871 https://doi.org/10.1144/GSL.MEM.2006.032.01.22, 2006.
872 Meissner, R., Wever, T., and Bittner, R.: Results of DEKORP 2-S and other reflection profiles through
873 the Variscides, Geophys J Int, 89, 319–324, https://doi.org/10.1111/j.1365-246X.1987.tb04425.x,
874 1987.
875 Meyer, R. K. F.: Der Jura in der Forschungsbohrung Obernsees, Geologica Bavarica, 88, 131–135,
876 available at: https://www.lfu.bayern.de/geologie/geo_karten_schriften/schriften/index.htm,
877 1985.
878 Müller, M.: Neue Vorstellungen zur Entwicklung des Nordostbayerischen Permokarbon-Trogs
879 aufgrund reflexionsseismischer Messungen in der Mittleren Oberpfalz, Geologische Blätter von
880 Nordost-Bayern, 44, 195–224, 1994.
881 Navabpour, P., Malz, A., Kley, J., Siegburg, M., Kasch, N., and Ustaszewski, K.: Intraplate brittle
882 deformation and states of paleostress constrained by fault kinematics in the central German
883 platform, Tectonophysics, 694, 146–163, https://doi.org/10.1016/j.tecto.2016.11.033, 2017.
884 Norton, M. G., McClay, K. R., and Way, N. A.: Tectonic evolution of Devonian basins in northern
885 Scotland and southern Norway, NJG, 67, 323–338, available at: http://njg.geologi.no/vol-61-
886 70/details/19/712-712, 1987.
887 Osmundsen, P. T. and Andersen, T. B.: The middle Devonian basins of western Norway: sedimentary
888 response to large-scale transtensional tectonics?, Tectonophysics, 332, 51–68,
889 https://doi.org/10.1016/S0040-1951(00)00249-3, available at:
890 https://www.sciencedirect.com/science/article/pii/S0040195100002493, 2001.
891 Patruno, S., Reid, W., Berndt, C., and Feuilleaubois, L.: Polyphase tectonic inversion and its role in
892 controlling hydrocarbon prospectivity in the Greater East Shetland Platform and Mid North Sea
893 High, UK, Geological Society, London, Special Publications, 471, 177,
894 https://doi.org/10.1144/SP471.9, 2019.
895 Paul, J.: Rotliegend und unterer Zechstein der Forschungsbohrung Lindau 1 (NE-Bayern), Geologica
896 Bavarica, 109, 27–48, 2006.
897 Paul, J. and Schröder, B.: Rotliegend im Ostteil der Süddeutschen Scholle, in: Innervariscische
898 Becken, edited by: Lützner, H., Schweizerbart Science Publishers, Stuttgart, Germany, 697–706,
899 2012.
900 Peterek, A., Rauche, H., Schröder, B., Franzke, H.-J., Bankwitz, P., and Bankwitz, E.: The late-and post-
901 Variscan tectonic evolution of the Western Border fault zone of the Bohemian massif (WBZ),
902 Geologische Rundschau, 86, 191–202, https://doi.org/10.1007/s005310050131, available at:
903 https://doi.org/10.1007/s005310050131, 1997.
904 Peterek, A., Rauche, H., and Schröder, B.: Die strukturelle Entwicklung des E-Randes der
905 Süddeutschen Scholle in der Kreide, Zeitschrift für Geologische Wissenschaften, 24, 65–77,
906 1996a.
907 Peterek, A., Schröder, B., and Menzel, D.: Zur postvariszischen Krustenentwicklung des Naabgebirges
908 und seines Rahmens, Zeitschrift für Geologische Wissenschaften, 24, 293–304, 1996b.
909 Peterek, A., Schröder, B., and Menzel, D.: Zur postvariszischen Krustenentwicklung des Naabgebirges
910 und seines Rahmens, Zeitschrift für Geologische Wissenschaften, 24, 293–304, 1996c.

https://doi.org/10.5194/se-2021-95
Preprint. Discussion started: 2 August 2021

911 Phillips, T. B., Fazlikhani, H., Gawthorpe, R. L., Fossen, H., Jackson, C. A.-L., Bell, R. E., Faleide, J. I.,
912 and Rotevatn, A.: The Influence of Structural Inheritance and Multiphase Extension on Rift
913 Development, the NorthernNorth Sea, Tectonics, n/a, https://doi.org/10.1029/2019TC005756,
914 2019.
915 Phillips, T. B., Jackson, C. A.-L., Bell, R. E., Duffy, O. B., and Fossen, H.: Reactivation of intrabasement
916 structures during rifting: A case study from offshore southern Norway, Journal of Structural
917 Geology, 91, 54–73, https://doi.org/10.1016/j.jsg.2016.08.008, 2016.
918 Platt, N. H. and Cartwright, J. A.: Structure of the East Shetland Platform, northern North Sea,
919 Petroleum Geoscience, 4, 353, https://doi.org/10.1144/petgeo.4.4.353, 1998.
920 Ravidà, D. C. G., Caracciolo, L., Henares, S., Janßen, M., and Stollhofen, H.: Drainage and
921 environmental evolution across the Permo–Triassic boundary in the south-east Germanic Basin
922 (north-east Bavaria), Sedimentology, n/a, https://doi.org/10.1111/sed.12913, 2021.
923 Ring, U.: The influence of preexisting structure on the evolution of the Cenozoic Malawi rift (East
924 African rift system), Tectonics, 13, 313–326, https://doi.org/10.1029/93TC03188, 1994.
925 Schröder, B.: Outline of the Permo-Carboniferous Basins at the Western Margin of the Bohemian
926 Massif, Zeitschrift für Geologische Wissenschaften, 16, 993–1001, 1988.
927 Schröder, B.: Inversion tectonics along the Western margin of the Bohemian Massif, Tectonophysics,
928 137, 93–100, https://doi.org/10.1016/0040-1951(87)90316-7, available at:
929 http://www.sciencedirect.com/science/article/pii/0040195187903167, 1987.
930 Schuh, H.: Der Zechstein in der Forschungsbohrung Obernsees, Geologica Bavarica, 88, 57–68, 1985.
931 Schwan, W.: Die sächsischen Zwischengebirge und Vergleiche mit der Münchberger Gneismasse und
932 anderen analogen Kristallinvorkommen im Saxothuringikum, Erlanger geologische
933 Abhandlungen, Heft 99, Erlangen: s.n, 180 p. 11 leaves of plates, 1974.
934 Scwan, W.: Die Säichsischen Zwischengebirge und Vergleiche mit der Münchberger Gneismasse und
935 anderen analogen Kristallinvorkommen im Saxothuringikum., Erlanger geologische
936 Abhandlungen, 99, 1974.
937 Séranne, M.: Devonian extensional tectonics versus Carboniferous inversion in the northern
938 Orcadian basin, Journal of the Geological Society, 149, 27,
939 https://doi.org/10.1144/gsjgs.149.1.0027, 1992.
940 Séranne, M. and Séguret, M.: The Devonian basins of western Norway: tectonics and kinematics of
941 an extending crust, Geological Society, London, Special Publications, 28, 537,
942 https://doi.org/10.1144/GSL.SP.1987.028.01.35, 1987.
943 Sitting, E. and Nitsch, E.: Stefan und Rotliegend zwichen Odenwald und Alpenrand, in:
944 Innervariscische Becken, edited by: Lützner, H., Schweizerbart Science Publishers, Stuttgart,
945 Germany, 646–696, 2012.
946 Specht, S.: Eltmann well description: Internal report, Bayerisches Landesamt fuer Umwelt, 2018.
947 STD: Die Stratigraphische Tabelle von Deutschland, 2016.
948 Stephan, T., Kroner, U., Hahn, T., Hallas, P., and Heuse, T.: Fold/cleavage relationships as indicator
949 for late Variscan sinistral transpression at the Rheno-Hercynian–Saxo-Thuringian boundary zone,
950 Central European Variscides, Tectonophysics, 681, 250–262,
951 https://doi.org/10.1016/j.tecto.2016.03.005, available at:
952 http://www.sciencedirect.com/science/article/pii/S004019511600161X, 2016.
953 Stephenson, R. A., Narkiewicz, M., Dadlez, R., van Wees, J.-D., and Andriessen, P.: Tectonic
954 subsidence modelling of the Polish Basin in the light of new data on crustal structure and
955 magnitude of inversion, Sedimentary Geology, 156, 59–70, https://doi.org/10.1016/S0037-
956 0738(02)00282-8, available at:
957 https://www.sciencedirect.com/science/article/pii/S0037073802002828, 2003.

https://doi.org/10.5194/se-2021-95
Preprint. Discussion started: 2 August 2021

958 Stettner, G.: Metamorphism and Tectonics in the Münchberg Mass and the Fichtelgebirge,
959 Fortschritte der Mineralogie, 52, 59–69, 1974.
960 Stettner, G. and Salger, M.: Das Schiefergebirge in der Forschungsbohrung Obernsees, Geologica
961 Bavarica, 88, 49–55, 1985.
962 Stollhofen, H.: Facies architecture variations and seismogenic structures in the Carboniferous–
963 Permian Saar–Nahe Basin (SW Germany): evidence for extension-related transfer fault activity,
964 Sedimentary Geology, 119, 47–83, https://doi.org/10.1016/S0037-0738(98)00040-2, available at:
965 https://www.sciencedirect.com/science/article/pii/S0037073898000402, 1998.
966 Strugale, M., Da Schmitt, R. S., and Cartwright, J.: Basement geology and its controls on the
967 nucleation and growth of rift faults in the northern Campos Basin, offshore Brazil, Basin Res, n/a,
968 https://doi.org/10.1111/bre.12540, 2021.
969 Trusheim, F.: Über den Untergrund Frankens; Ergebnisse von Tief Bohrungen in Franken und
970 Nachbargebieten, Geologica Bavarica, 54, 1–106, 1964.
971 Vasconcelos, D. L., Bezerra, F. H., Medeiros, W. E., Castro, D. L. de, Clausen, O. R., Vital, H., and
972 Oliveira, R. G.: Basement fabric controls rift nucleation and postrift basin inversion in the
973 continental margin of NE Brazil, Tectonophysics, 751, 23–40,
974 https://doi.org/10.1016/j.tecto.2018.12.019, 2019.
975 Vetti, V. V. and Fossen, H.: Origin of contrasting Devonian supradetachment basin types in the
976 Scandinavian Caledonides, Geology, 40, 571–574, https://doi.org/10.1130/G32512.1, 2012.
977 Wagner, G. A., Coyle, D. A., Duyster, J., Henjes-Kunst, F., Peterek, A., Schröder, B., Stöckhert, B.,
978 Wemmer, K., Zulauf, G., Ahrendt, H., Bischoff, R., Hejl, E., Jacobs, J., Menzel, D., Lal, N., van den
979 Haute, P., Vercoutere, C., and Welzel, B.: Post-Variscan thermal and tectonic evolution of the KTB
980 site and its surroundings, J. Geophys. Res., 102, 18221–18232,
981 https://doi.org/10.1029/96JB02565, 1997.
982 Wemmer, K.: K-Ar-Altersdatierungsmöglichkeiten für retrograde Deformationsprozesse im spröden
983 und duktilen Bereich-Beispiele aus der KTB -Vorbohrung (Oberpfalz) und dem Bereich der
984 Insubrischen Linie (N-Italien)., Göttinger Arbeiten Zur Geologie und Paläontologie, 51, 1–61,
985 1991.
986 Wever, T., Meissner, R., and Sadowiak, P.: Deep reflection seismic data along the central part of the
987 European Geotraverse in Germany: a review, Tectonophysics, 176, 87–101,
988 https://doi.org/10.1016/0040-1951(90)90260-F, available at:
989 http://www.sciencedirect.com/science/article/pii/004019519090260F, 1990.
990 Wiest, J. D., Wrona, T., Bauck, M. S., Fossen, H., Gawthorpe, R. L., Osmundsen, P. T., and Faleide, J. I.:
991 From Caledonian Collapse to North Sea Rift: The Extended History of a Metamorphic Core
992 Complex, Tectonics, 39, e2020TC006178, https://doi.org/10.1029/2020TC006178, 2020.
993 Wrona, T., Fossen, H., Lecomte, I., Eide, C. H., and Gawthorpe, R. L.: Seismic expression of shear
994 zones: Insights from 2-D point-spread-function-based convolution modelling, Geol, 104121,
995 https://doi.org/10.1016/j.jsg.2020.104121, available at:
996 http://www.sciencedirect.com/science/article/pii/S0191814119303037, 2020.
997 Ye, Q., Mei, L., Shi, H., Du, J., Deng, P., Shu, Y., and Camanni, G.: The Influence of Pre-existing
998 Basement Faults on the Cenozoic Structure and Evolution of the Proximal Domain, Northern
999 South China Sea Rifted Margin, Tectonics, 39, e2019TC005845,
1000 https://doi.org/10.1029/2019TC005845, 2020.
1001 Ziegler, P. A.: Tectonic and palaeogeographic development of the North Sea rift system, Tectonic
1002 Evolution of North Sea Rifts, 1–36, 1990.
1003
1004
1005

https://doi.org/10.5194/se-2021-95
Preprint. Discussion started: 2 August 2021

Figure and Table caption

Figure 1: Location of the study are in the Saxothuringian zone of Variscan orogeny. FRANKEN seismic survey is projected on geological map of the study area in dark red creating a grid of 2D seismic profiles with existing DEKORP profiles. Main Faults are shown as bold dark lines. Inset map shows exposed Variscan terranes in Central Europe. Yellow circles show deep wells in the study area. FRA: FRANKEN, MGCH: Mid German Crystalline High, FFS: Franconian Fault System and MN: Münchberg Nappe.

Figure 2: Velocity and density logs from well Mürsbach 1 utilized for synthetic seismogram generation. Seismic traces from FRANKEN-1802 are compared with generated synthetic seismogram. Velocity data are used to construct time-depth relationship and well-seismic ties. Depth to the formation tops are time converted and used as starting point for seismic interpretation.

Figure 3: Seismo-stratigraphic facies of observed Permian-Jurassic stratigraphy in the study area. A) Jurassic, B) Upper Triassic Keuper Group, c) Middle Triassic Muschelkalk Group, D) Lower Triassic Buntsandstein Group and D) Permian Zechstein and Rotliegend Groups.

Figure 4: Basement Seismic Facies (BSF) described along FRANKEN seismic survey. A) shows SE portion of FRANKEN-1804 below the Top Zechstein horizon. B) Low-amplitude and discontinuous reflections of BSF1 interpreted as Paleozoic metasedimentary rocks and Variscan nappe units. C) BSF2 shows high-amplitude, continuous and dipping reflection interpreted as Variscan shear zones. D) Medium-amplitude and semi-continuous reflections of BSF3 below Variscan shear zone related to the Saxothuringian basement.

Figure 5: Repossessed DEKORP-85 4N and DEKORP-3/MVE-90 profiles used to compare three Basement Seismic Facies (BSF1-3) described along FRANKEN seismic survey (see Fig. 1 for location). DEKORP profiles image exposed Variscan units along the western Bohemian Massif and are used as proxy for geological interpretation of BSFs. A) DEKORP-85 4N shows seismic signature of Paleozoic low-grade metasedimentary rocks (zoomed in B) and Münchberg Nappe (Variscan allochthon, zoomed in C) exposed at the surface and described as BSF1. D) DEKORP-3/MVE-90 images Münchberg nappe units east and Permian-Jurassic sedimentary cover west of Franconian Fault System (FFS). E) shows seismic signature of Variscan nappes (BSF1) and underlying shear zones (BSF2).

Figure 6: A) uninterpreted and B) interpreted FRANKEN-1801 profile. Horizon interpretation is tied to drilled wells in the study area. C) geo-seismic section in time (ms TWT), and D) depth converted profile with no vertical exaggeration. Intersecting profiles FRANKEN 1802 and 1804 are shown by black arrows. See Figure 1 for the profile location.

Figure 7: Profile FRNKEN-1802 strikes NE-SW, perpendicular to main structures. A) uninterpreted and B) interpreted seismic profile. FRANKEN-1802 is tied to well Eltmann, Mürsbach, Staffelstein 1 and 2. High-amplitude and continuous reflection of BSF2 interpreted as Variscan shear zones are at 2000-2500 ms TWT (5-6.5 km) in the NE and reach to the base of Permian sedimentary rocks to the SE. C) geo-seismic section in time with vertical exaggeration of 5. D) depth converted section with no vertical exaggeration. See Figure 1 for the profile location.

Figure 8: SE-NW striking FRANKEN-1803 profile, sub-parallel to the profile FRANKEN-1801. Horizon interpretation is tied to well Obernsees and intersection FRANKEN 1801 and 1804 profiles. A) uninterpreted and B) interpreted profile. C) geo-seismic section in time and D) depth converted section with not vertical exaggeration. Interpreted Variscan shear zones (BSF2) are at 2000-3000 ms (5-7 km) in the SE and reaches to ca. 2.5 km depth towards NW.

https://doi.org/10.5194/se-2021-95
Preprint. Discussion started: 2 August 2021

Figure 9: A) uninterpreted and B) interpreted profile FRANKEN-1804. Horizon interpretation along this profile is tied to intersection profiles FRANKEN 1801 and 1803. Note onlapping reflections in the hanging wall of SW-dipping normal faults creating Permian half-grabens. C) geo-seismic section in time and D) depth converted section with no vertical exaggeration. See Figure 1 for the profile location.

Figure 10: Present day three-dimensional view of interpreted Variscan units and structures west of Franconian Fault System (FFS). Variscan shear zone shows syn and antiformal geometries shallowing and thinning toward the W-SW.

Figure 11: Simplified cartoons showing the relationships between orogenic structures and post-orogenic fault and basin development. At the latest orogenic and early post-orogenic period, normal faults develop along preexisting orogenic structures as well as away from the orogenic structures. Some of the normal faults detach into the underlying shear zones. Geometry of underlying shear zones may localize the strain and facilitate fault initiation. Initiated normal faults grow laterally and vertically and initiate graben and half-graben basins in their hanging wall side. After a Triassic and Jurassic regional tectonic quiescence, Cretaceous inversion event in Central Europe selectively reactivate Permian normal faults as steep reverse faults, exposing older stratigraphy in the hinging wall side and creating local syn and anticlines in the vicinity of reactivated faults.

Table 1: Deep wells in the study area with formation tops used in seismic horizon interpretation of FRANKEN seism survey. See figure 1 for well location.

Table 2: Recording parameters of FRNAKEN seismic survey.

https://doi.org/10.5194/se-2021-95
Preprint. Discussion started: 2 August 2021

Solid Earth
Discussions
Open Access
EGU

Figure 01

https://doi.org/10.5194/se-2021-95
Preprint. Discussion started: 2 August 2021

Solid Earth
Discussions
Open Access
EGU

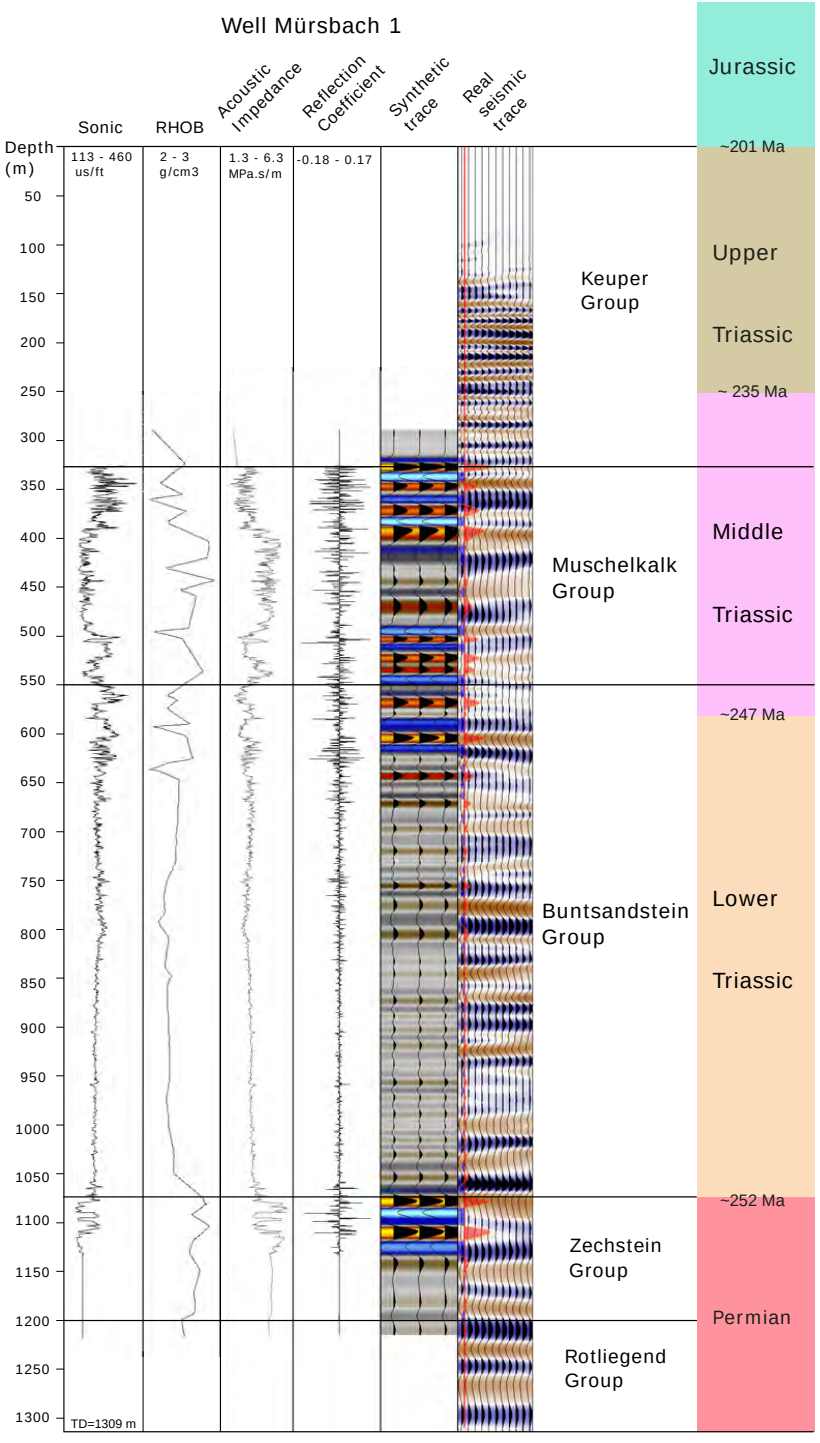

Figure 02

https://doi.org/10.5194/se-2021-95
Preprint. Discussion started: 2 August 2021

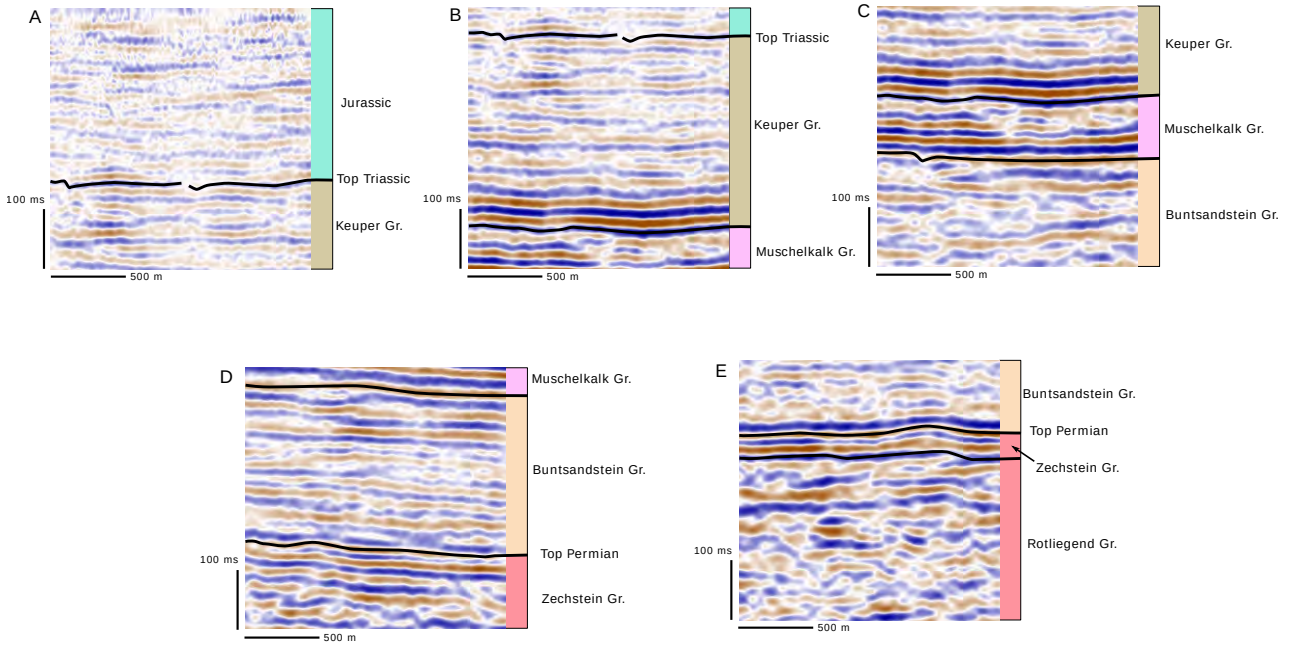

Figure 03

https://doi.org/10.5194/se-2021-95
Preprint. Discussion started: 2 August 2021

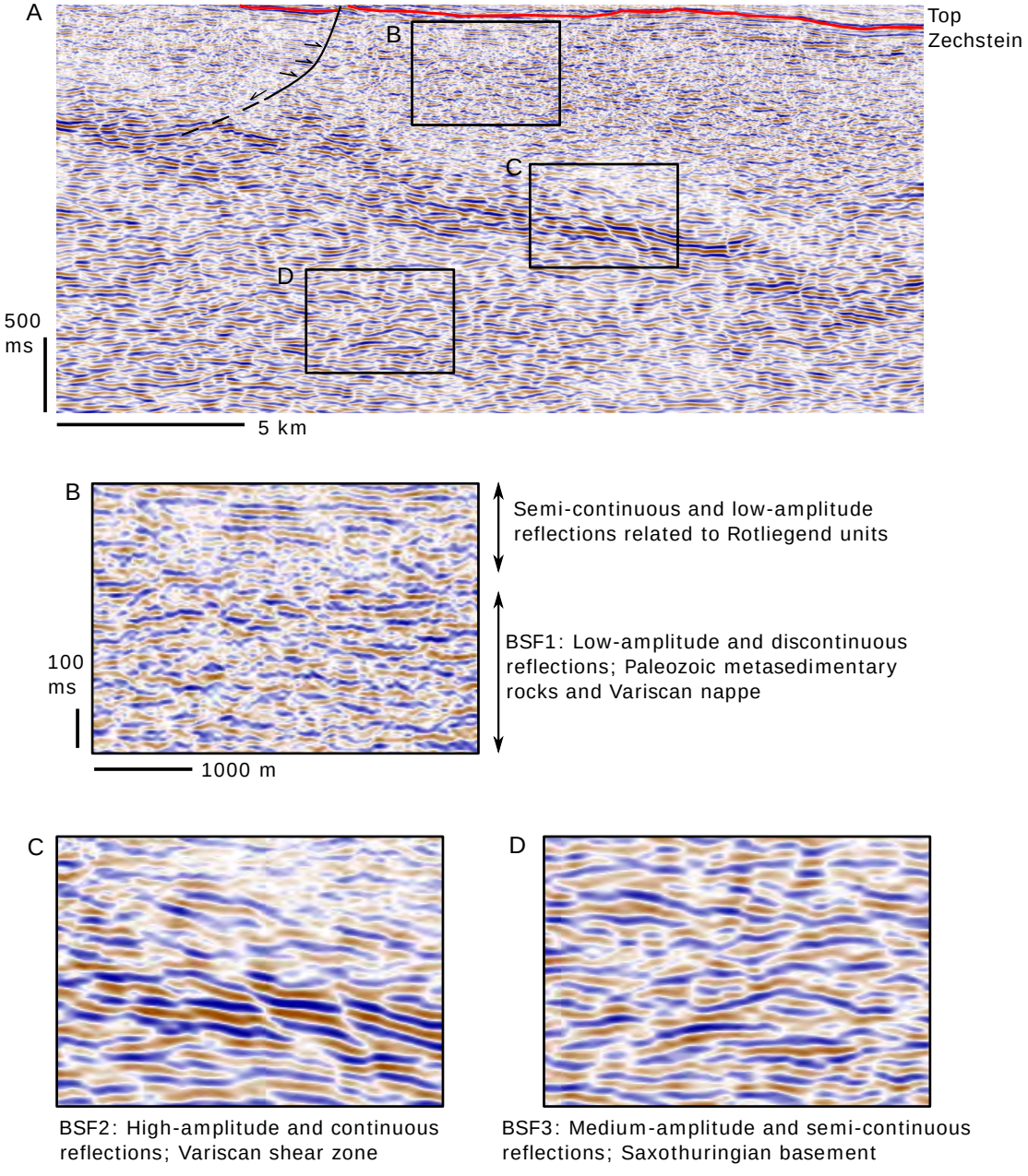

Figure 04

https://doi.org/10.5194/se-2021-95
Preprint. Discussion started: 2 August 2021

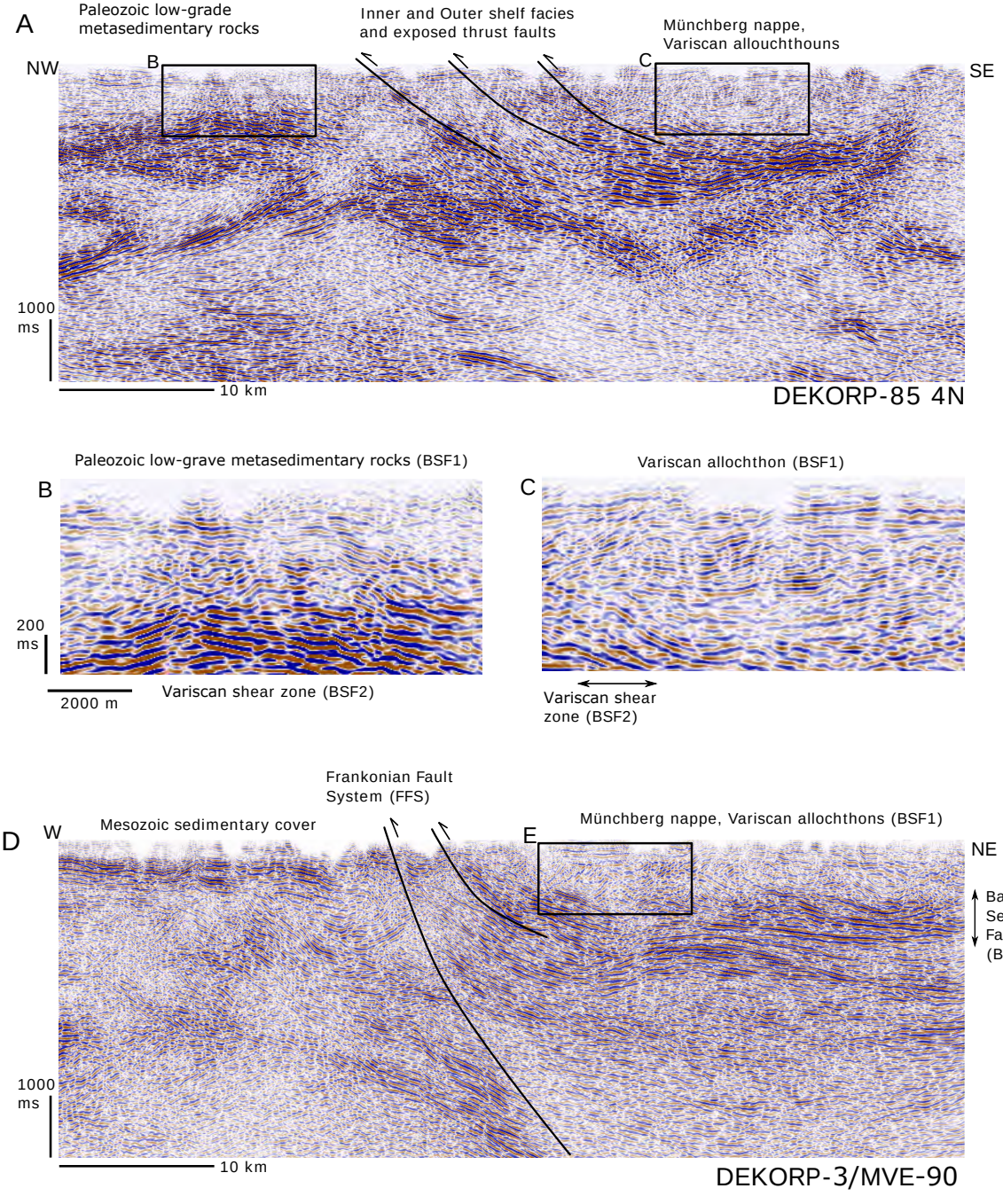

Figure 05

https://doi.org/10.5194/se-2021-95
Preprint. Discussion started: 2 August 2021

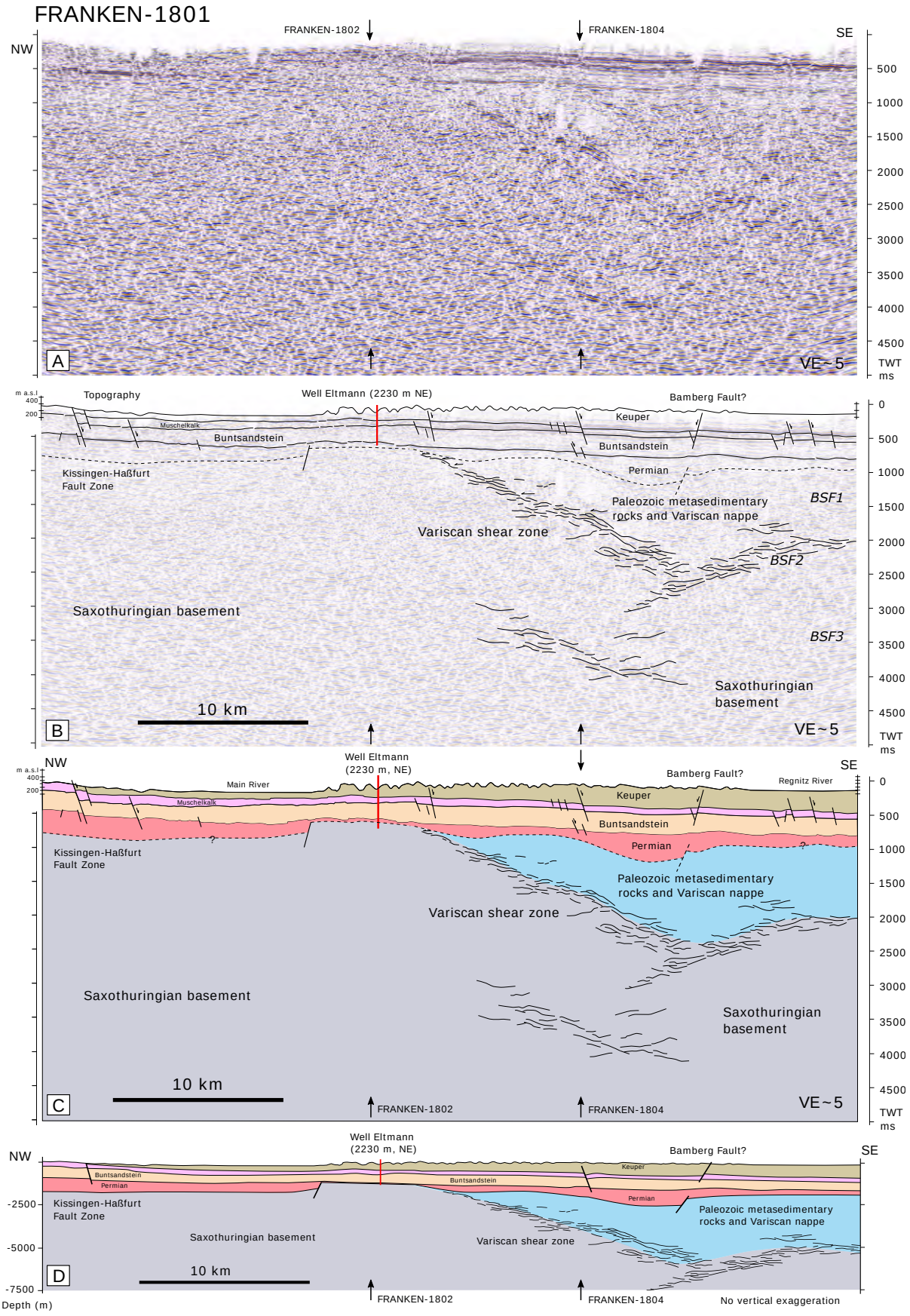

Figure 06

https://doi.org/10.5194/se-2021-95
Preprint. Discussion started: 2 August 2021

Solid Earth
Discussions
Open Access
EGU

Figure 07

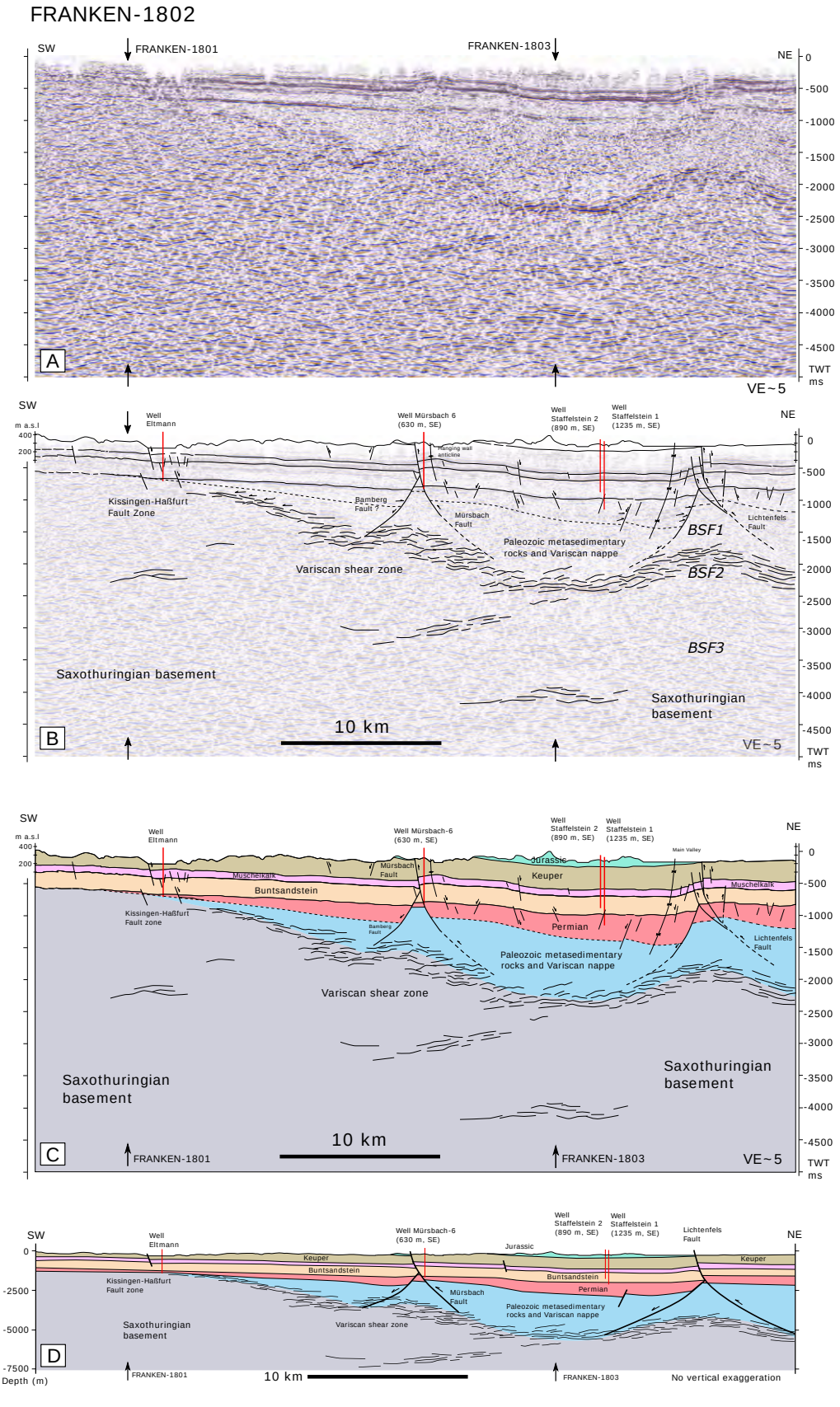

https://doi.org/10.5194/se-2021-95
Preprint. Discussion started: 2 August 2021

Solid Earth
Discussions
Open Access
EGU

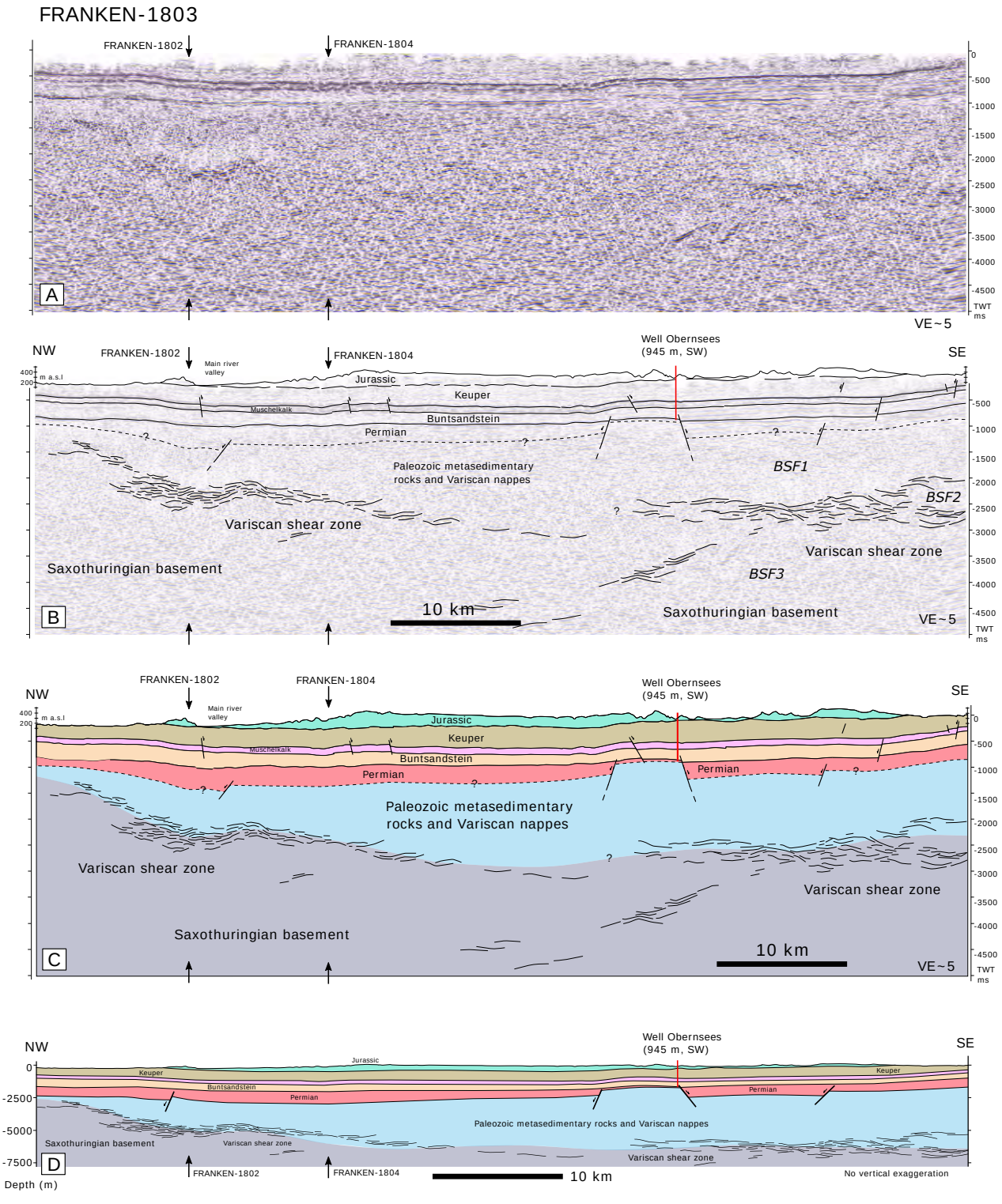

Figure 08

https://doi.org/10.5194/se-2021-95
Preprint. Discussion started: 2 August 2021

Solid Earth
Discussions
Open Access
EGU

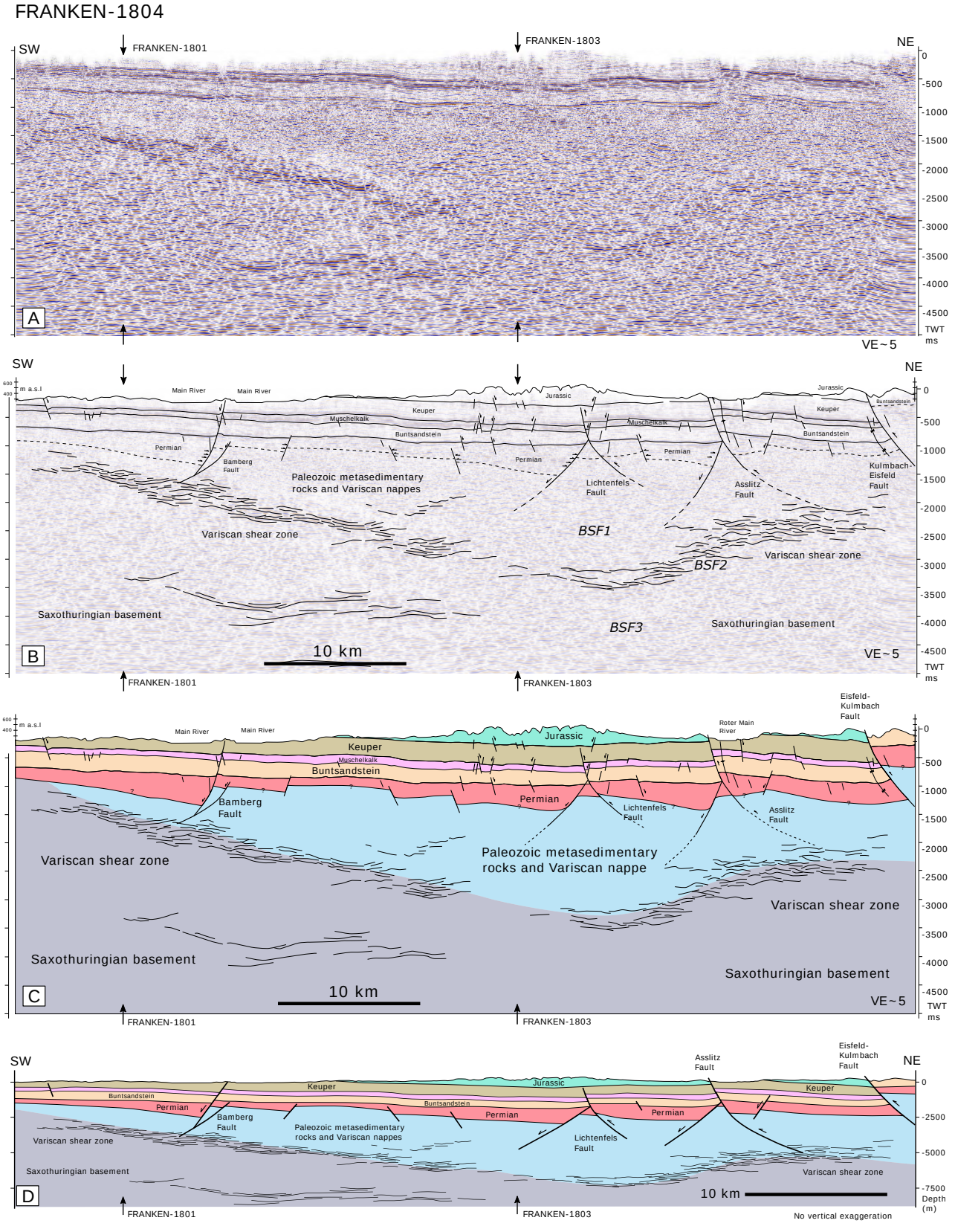

Figure 09

https://doi.org/10.5194/se-2021-95
Preprint. Discussion started: 2 August 2021

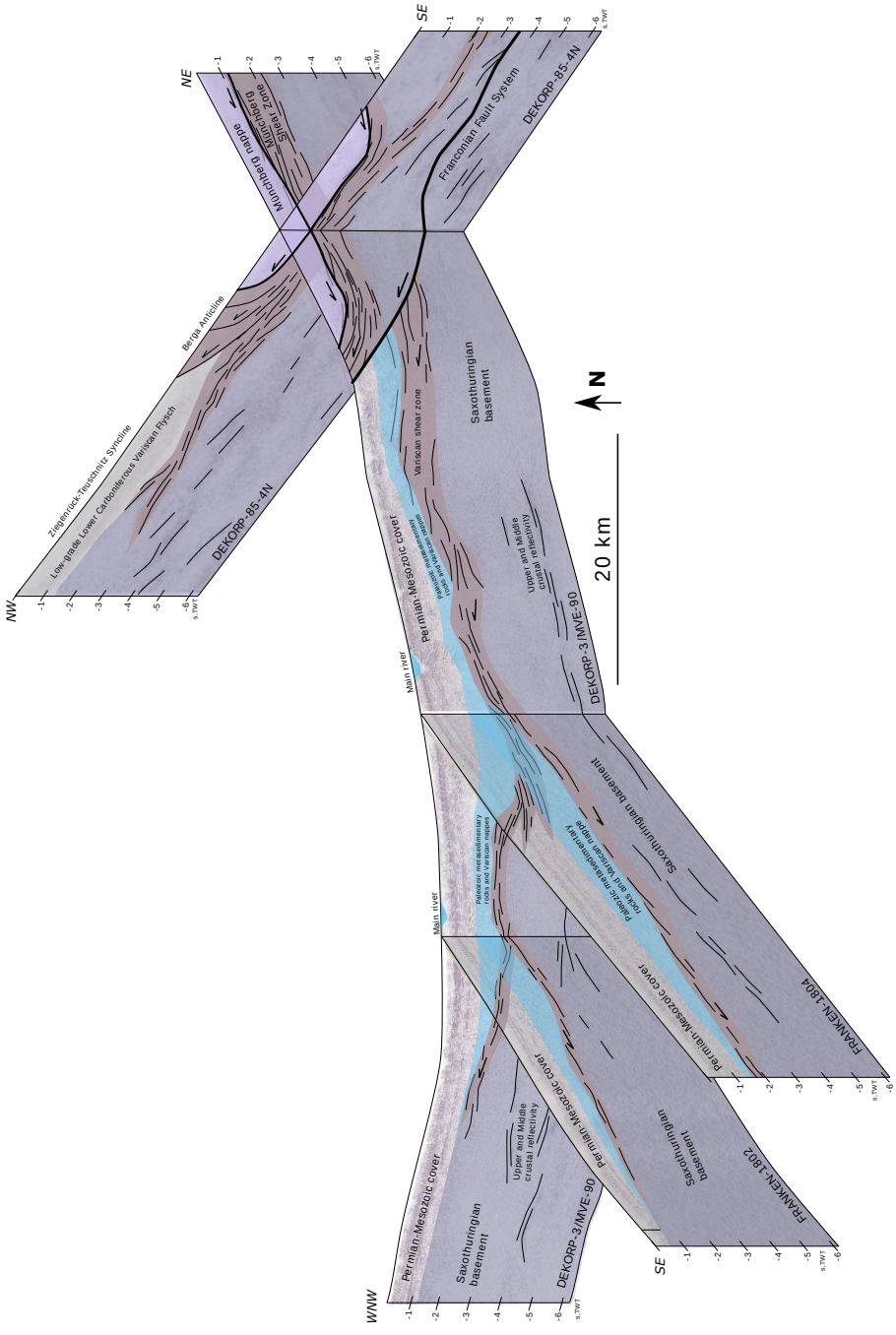

Figure 10

https://doi.org/10.5194/se-2021-95
Preprint. Discussion started: 2 August 2021

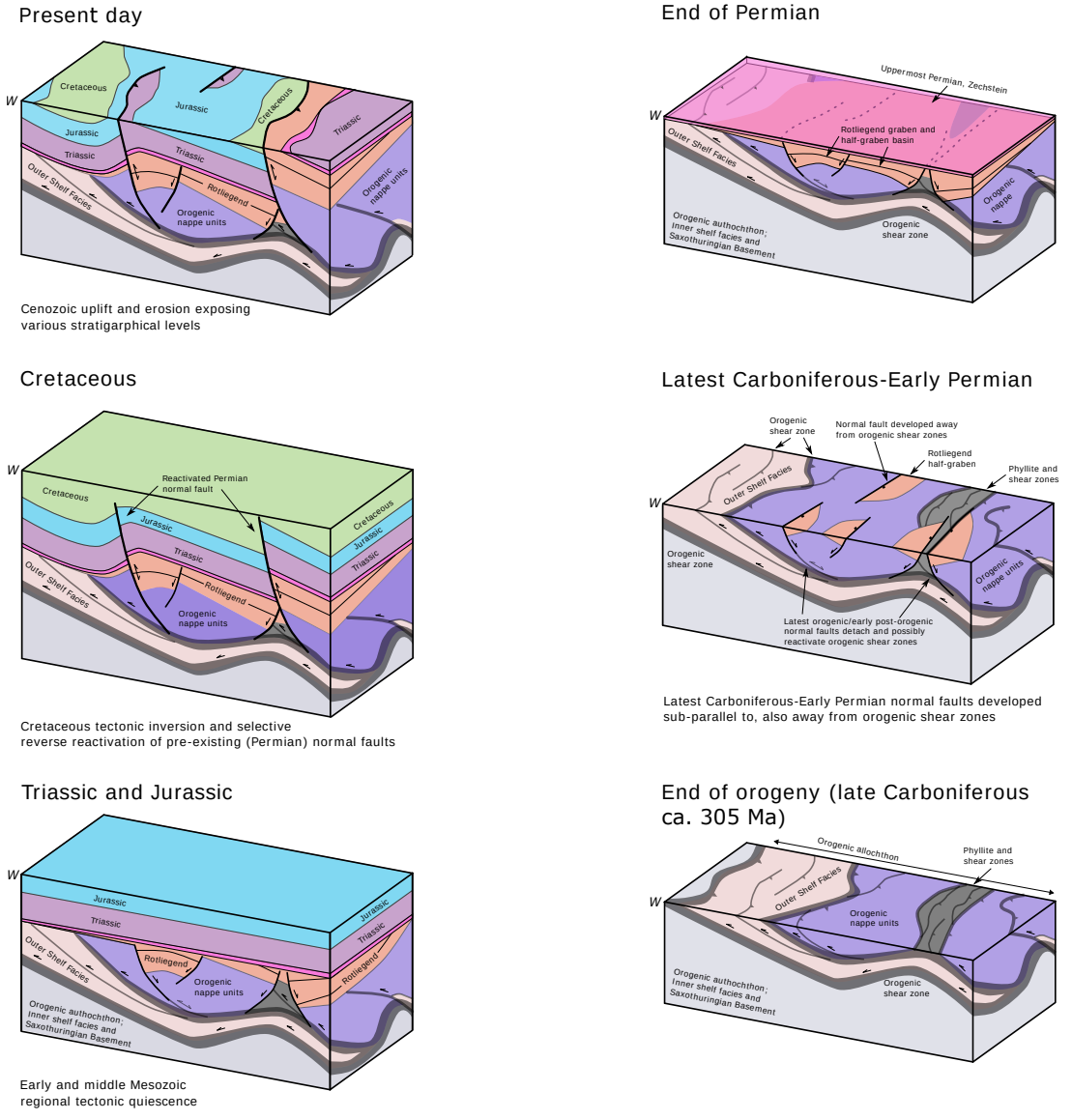

Figure 11

https://doi.org/10.5194/se-2021-95
Preprint. Discussion started: 2 August 2021

Solid Earth
Discussions
Open Access
EGU

Well	Quaternary	Jurassic	Keuper	Muschelkalk	Buntsandstein	Zechstein	Rotliegend	Basement	TD (m)
Obernsees	0	140	483	178.35	417.15	104.9	18.3	48.3	1390
Mürsbach 01	26	0	300	224	524	126	109	-	1309
Mürsbach 03	0	0	384.4	212.6	551	87	-	-	1235
Mürsbach 04	0	0	345.6	210.5	548.3	73.6	-	-	1178
Mürsbach 05	15.6	0	338.1	214.7	559	56.6	-	-	1184
Mürsbach 06	0	0	338.3	210.7	530.7	121.6	20.7	-	1222
Staffelstein 1	9	102	530.2	239.8	572.2	103.8	43	-	1600
Staffelstein 2	8	104	532	235	301	-	-	-	1180
Eltmann	9.4	0	178.6	235	510	114	3	94	1144
Lindau	0.25	0	0	0	182.05	98.05	250.25	-	530.6
Laineck	3.5	0	409.5	179	488	42	-	-	1122
Haarbrücken	6	0	0	0	199	109.5	185.4	-	499.9
Mittelberg	0	0	0	0	405.5	75.5	41.5	100.5	623
Bad Rodach 1	0	0	130	266	256	-	-	-	652
Bad Rodach 2	0	0	211.7	257.1	526.2	20	-	-	1015
Bad Königshofen	3.5	0	56.5	251	640	76	-	-	1027
Bad Colberg	18	0	322.5	224.5	555.5	157	123.5	-	1401
Wolfersdorf (Stockheim outcrop)	14	0	0	0	0	0	726	29.5	769.5

Table 01

https://doi.org/10.5194/se-2021-95
Preprint. Discussion started: 2 August 2021

Recording parameters

Number of profiles	4
FRANKEN-1801	47900 m, NW-SE
FRANKEN-1802	47750 m, NE-SW
FRNAKEN-1803	71800 m, NW-SE
FRANKEN-1804	63350 m, NE-SW
Method	Vibroseis
Number of channels	2400
Spread	Symmetrical split-spread with roll-in and roll-off
Active spread	800 stations (2.400 stations) full spread
Source	
P-wave source	Prakla-Seismos VVCA/E, 3 vibrators
Hydraulic peak force	13.500 da N
Source energy	28.000 lbs / 125 kN (nominal)
Weight	17.000 kg
Sweep length	16.000 ms
Sweep frequency range	8 - 64 Hz
Sweeps per VP	6
Sweep period	8-40 s
Vertical stacking	2 to 4
Recording	
Source point distance	100 m
Receiver point distance	12.5 m
Natural frequency	10 Hz
Geophone type	Sercel DSU-3, three component MEMS
Recording instrument	Sercel 428 XL
Recording length	8000 ms
Sampling rate	4 ms
Recording format	SEG-D, 8058

Table 02